CONTROL DE HURACANES SIMULADOS

Se recurre a modelos informáticos para simular dos huracanes devastadores de 1992, Iniki y Andrew. Los colores representan categorías de velocidad del viento. Las líneas de nivel negras indican vientos de 90 km/h; este valor viene a coincidir con el umbral de devastación del meteoro.

En las simulaciones de Iniki (*derecha*), la trayectoria original del ojo (*línea negra de trazos*) lleva los vientos más fuertes de la tempestad sobre la isla hawaiana de Kauai. Pero cuando varias de las condiciones iniciales del modelo, entre ellas la temperatura y humedad en diversos puntos, se alteraron ligeramente, la trayectoria simulada de la tempestad (*línea roja de trazos*) se desplazó hacia el oeste de Kauai, pasando sobre un blanco elegido a 97 kilómetros de la isla. Después siguió hacia el norte; llegó a un enclave de la isla más a su oeste que el huracán real.

Los mapas de los mares próximos a las Bahamas y Florida (*abajo*) muestran simulaciones de Andrew en su estado inalterado (*izquierda*) y en una forma artificialmente perturbada (*derecha*). Aunque los vientos catastróficos persisten en el caso controlado, las velocidades máximas se han reducido bastante: un huracán de categoría 3 se ha quedado en huracán de categoría 1, mucho menos brutal.

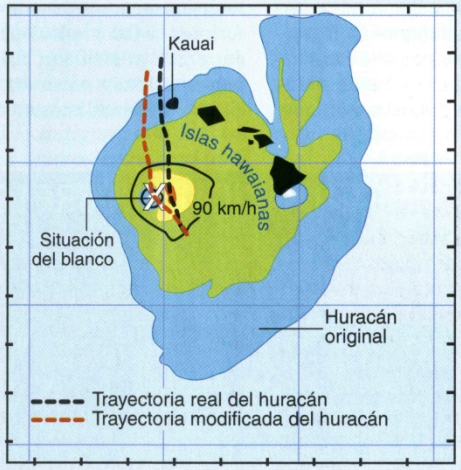

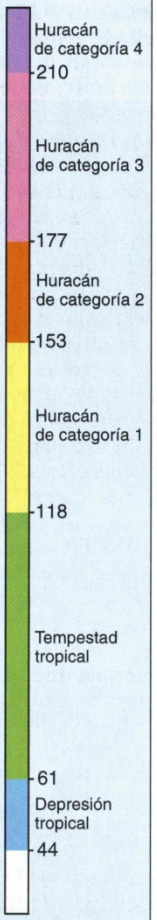

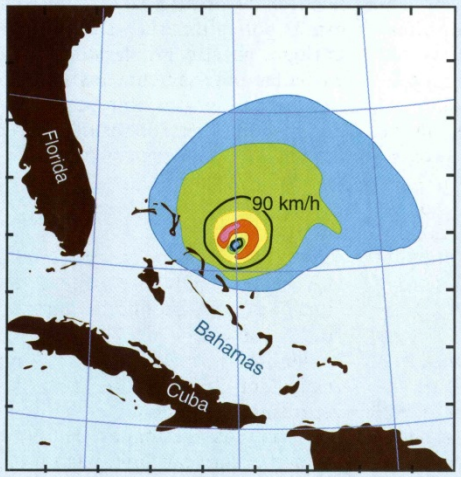

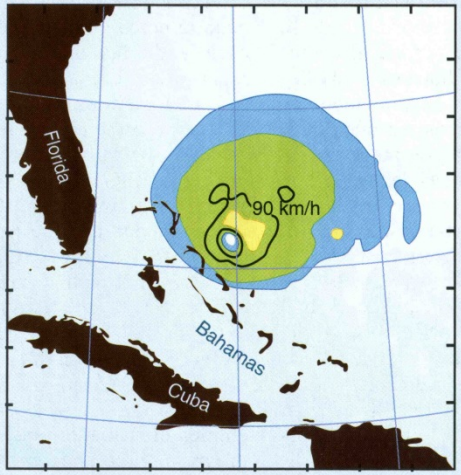

ACTUACIONES SOBRE LOS HURACANES

Las simulaciones informáticas de los huracanes indican que ciertas variaciones en la precipitación, evaporación y temperatura del aire podrían alterar la trayectoria de la tempestad o debilitar sus vientos. La actuación podría tomar varias formas: una siembra aérea de nubes, sobre objetivos meticulosamente seleccionados, con yoduro de plata u otros materiales inductores de precipitación podría servir para privar a la violenta pared del ojo del huracán —la característica fundamental de una gran tempestad tropical— del agua que necesita para crecer e intensificarse (*izquierda*). Se podría distribuir aceite biodegradable sobre la superficie del mar en la trayectoria del huracán para reducir la evaporación, que es la fuente de la energía de una tempestad (*centro*). Futuras estaciones orbitales de producción de electricidad mediante energía solar, que quizá recurran a grandes espejos para focalizar los rayos del sol y a paneles de células fotovoltaicas para cosechar esa energía y transferirla a la Tierra, emitirían microondas, sintonizadas de manera que las absorbiesen las moléculas de vapor de agua de la tempestad o sus alrededores (*derecha*). Las microondas harían vibrar las moléculas de agua y calentarían así el aire circundante. El huracán se debilitaría entonces o se movería en la dirección deseada.

Siembra: hielo seco, humo de yoduro de plata.,,

10:37 LST–16,100'

11:12 LST–14,250'
26 min. después de la inseminación

11:20 LST–16,100'
34 min. después de la inseminación

11:31 LST–16,200'
min. después de la inseminación

1972: Cambrige, EE.UU.

Trilogía

La “Trilogía Universal” de la Matemática Aplicada

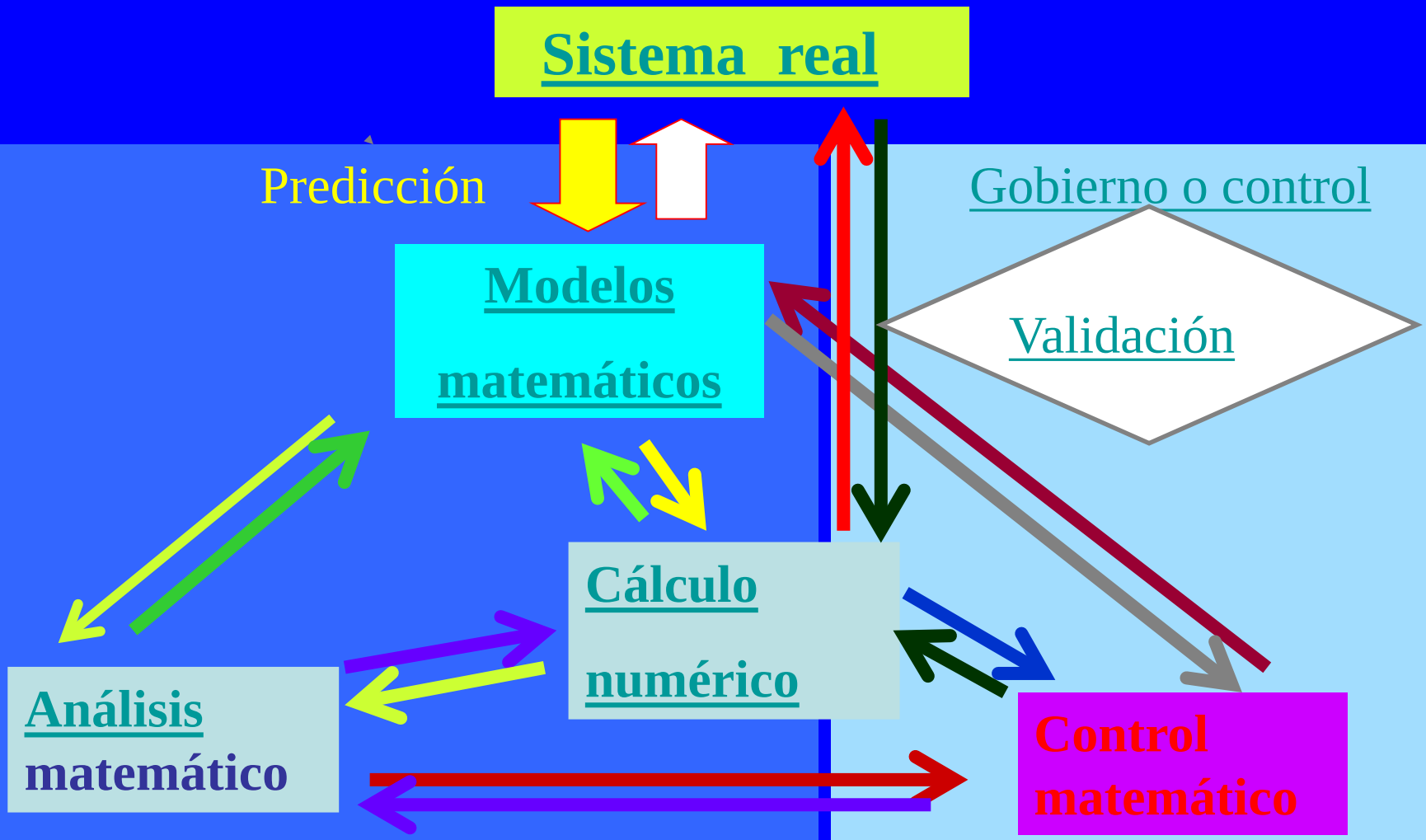

Teoría de Control / Teoría de juegos

- Estructura general:

  y=estado(s), u=control(es)

  - Ley de estado: $F(y_t, Ay, Bu)=0$ (A y B operadores)
  - Funcional de observabilidad: $J(u)=g(u,y(u))$

Problema: optimizar J(u) sobre un conjunto K de posibles controles

- Tª Control: u escalar (un único control)
- Tª de Juegos: u con múltiples componentes

  ¡Posible conflicto de intereses!

Planeta Tierra: sistema complejo

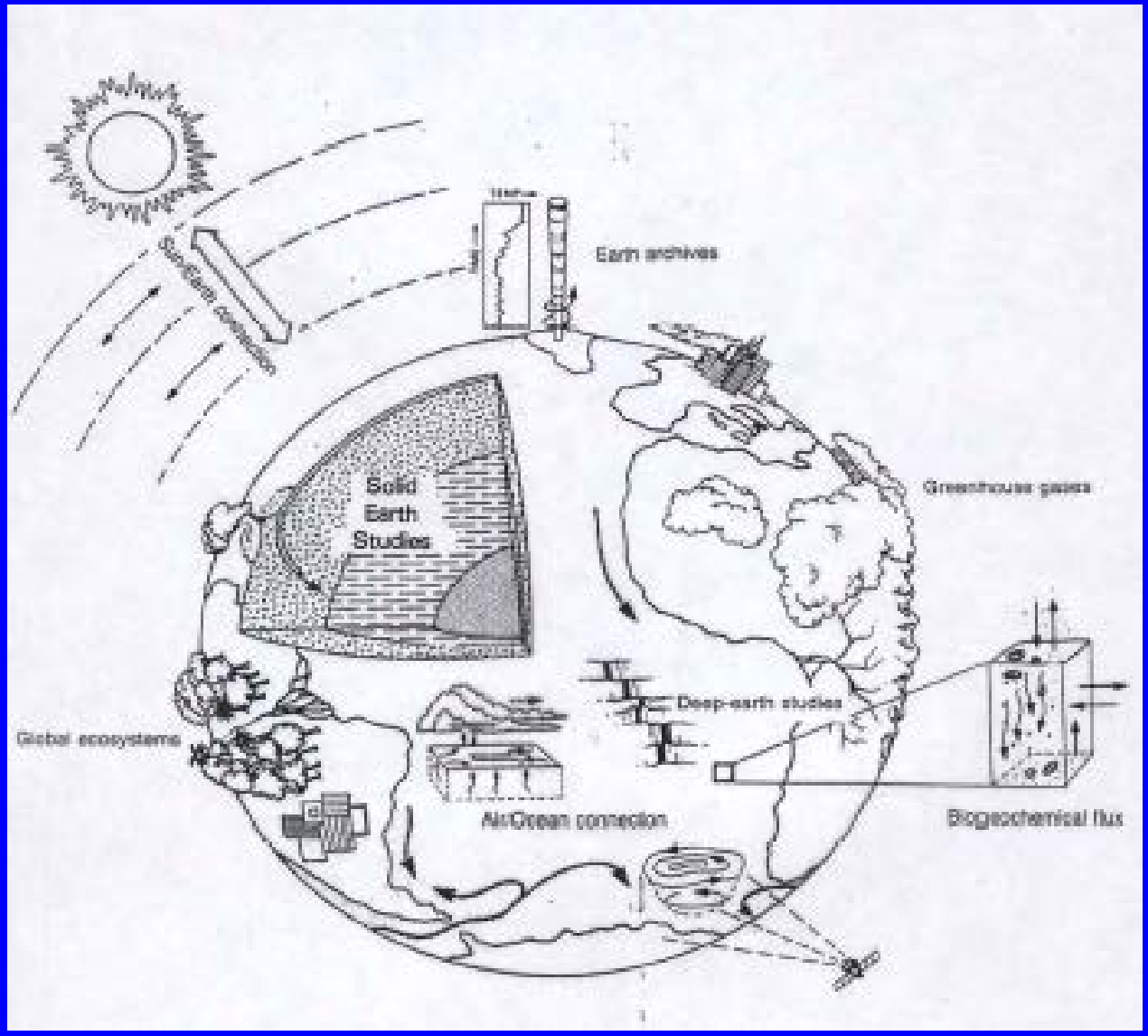

2. Materia: nuevos materiales.

Some motivations:

www.nature.com/nature

Vol 437|Issue no. 7059|29 September 2005

SURFACES AND INTERFACES

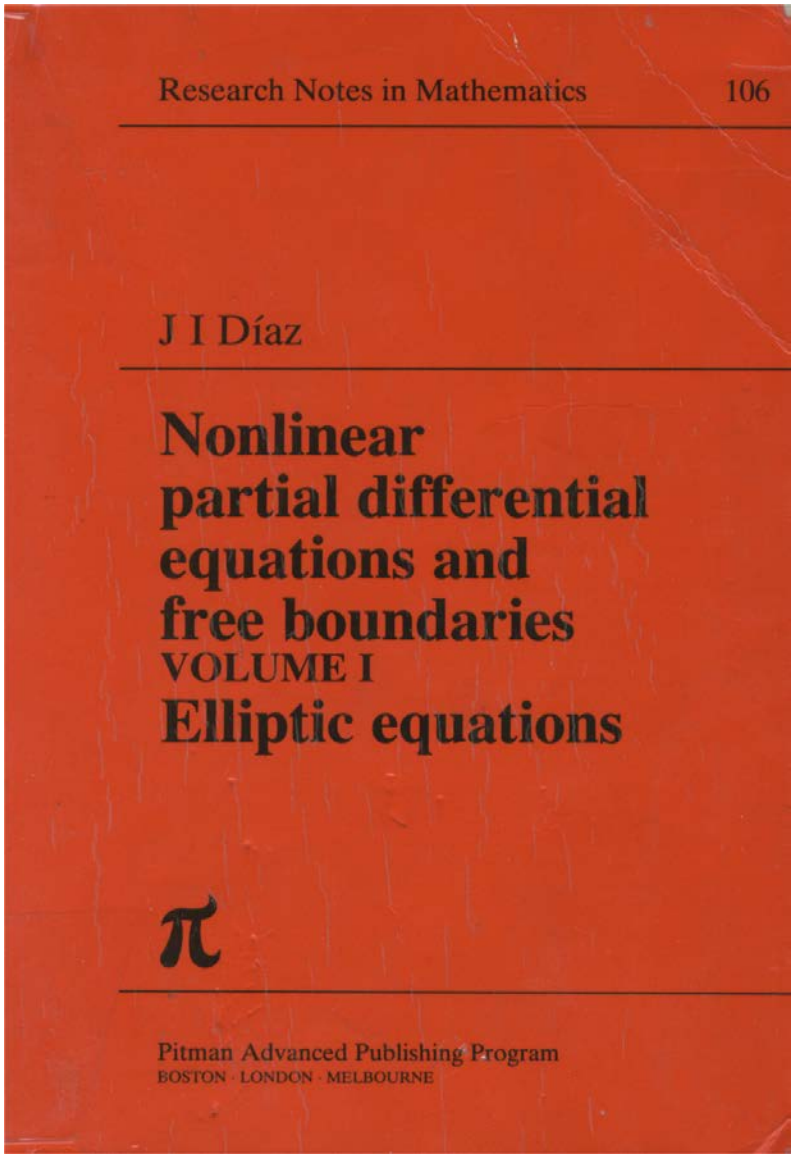
Research Notes in Mathematics 106
J I Díaz
Nonlinear partial differential equations and free boundaries
VOLUME I
Elliptic equations
π
Pitman Advanced Publishing Program
BOSTON · LONDON · MELBOURNE

1985

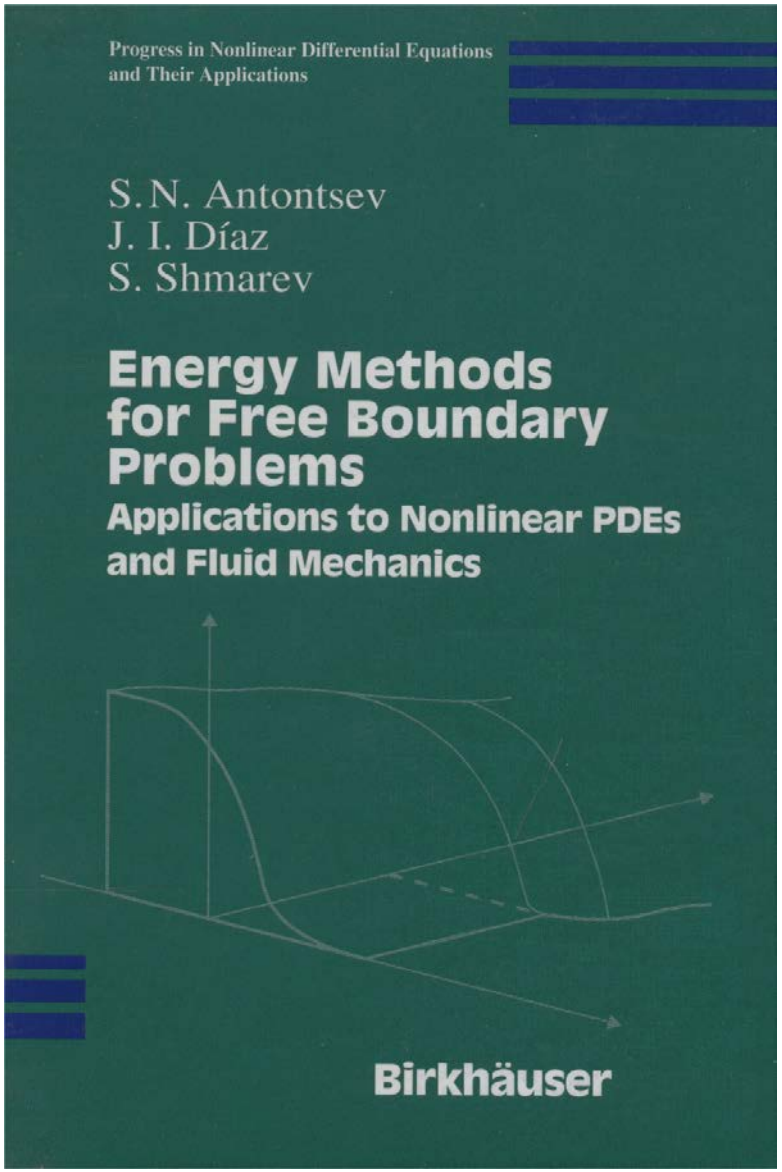
Progress in Nonlinear Differential Equations and Their Applications
S.N. Antontsev
J. I. Díaz
S. Shmarev
Energy Methods for Free Boundary Problems
Applications to Nonlinear PDEs and Fluid Mechanics
Birkhäuser

2002

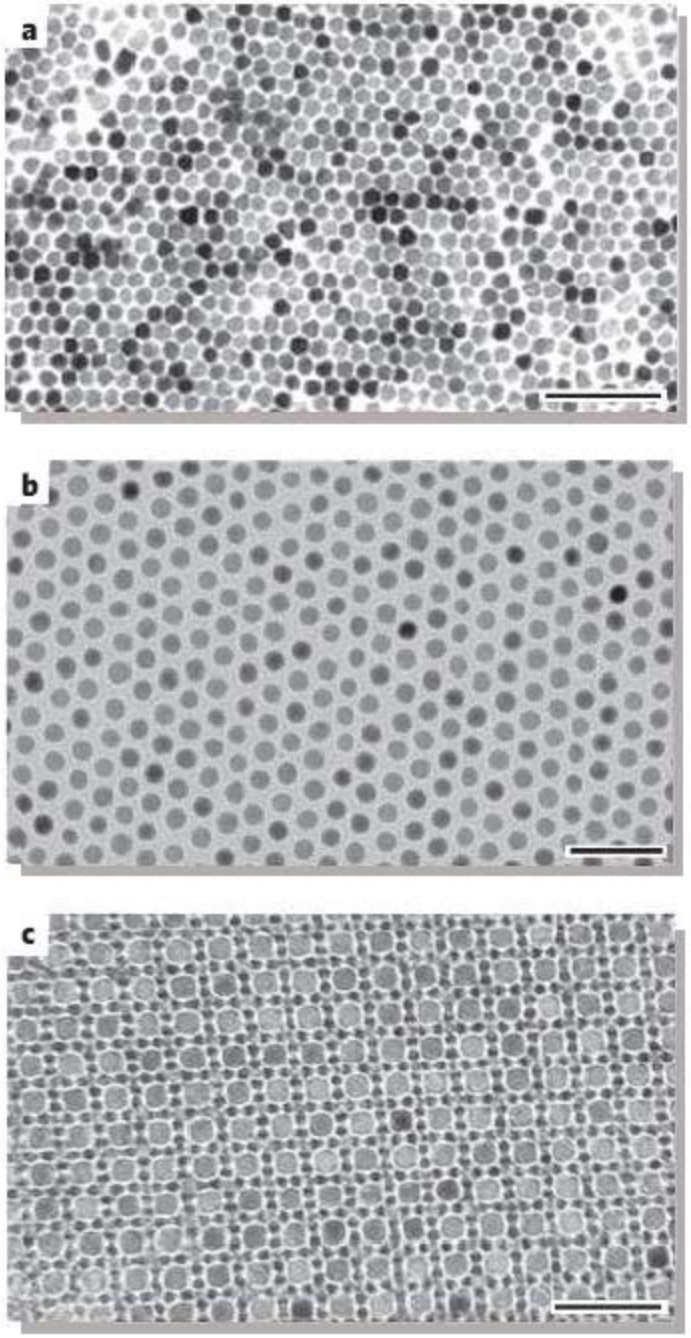

Figure 3 | Monodisperse colloidal nanocrystals synthesized under kinetic size control. **a**, Transmission electron microscopy (TEM) image of CdSe nanocrystals. **b**, TEM image of cobalt nanocrystals. **c**, TEM micrograph of an AB_{13} superlattice of γ-Fe_2O_3 and PbSe nanocrystals. The precise control on the size distributions of both nanocrystals allows their self-assembly into ordered three-dimensional superlattices. Scale bars, 50 nm. Reprinted from ref. 27.

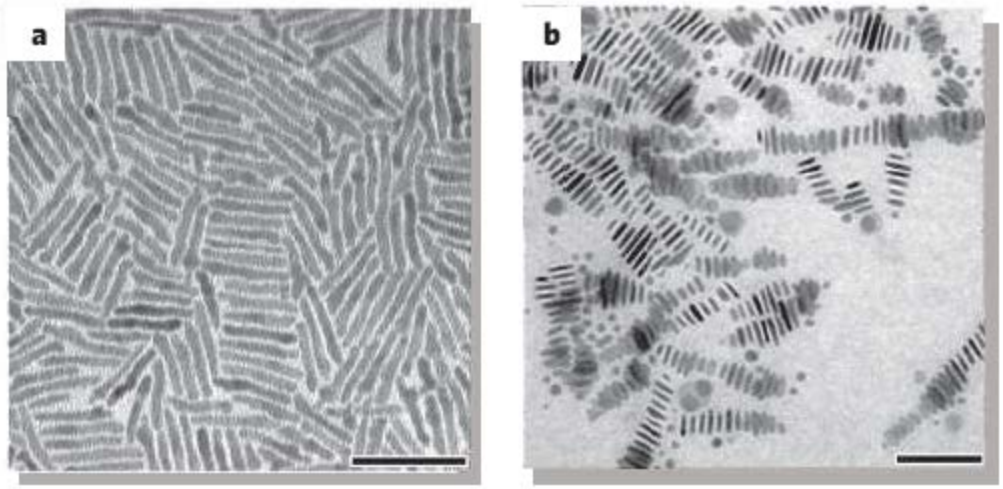

Figure 4 | Anisotropic growth of nanocrystals by kinetic shape control and selective adhesion. **a**, CdSe nanorods (scale bar, 50 nm). Reprinted with permission from ref. 52. **b**, Cobalt nanodisks (scale bar, 100 nm). The organic surfactant molecules selectively adhere to one facet of the nanocrystal, allowing the crystal to grow anisotropically to form a rod or disk.

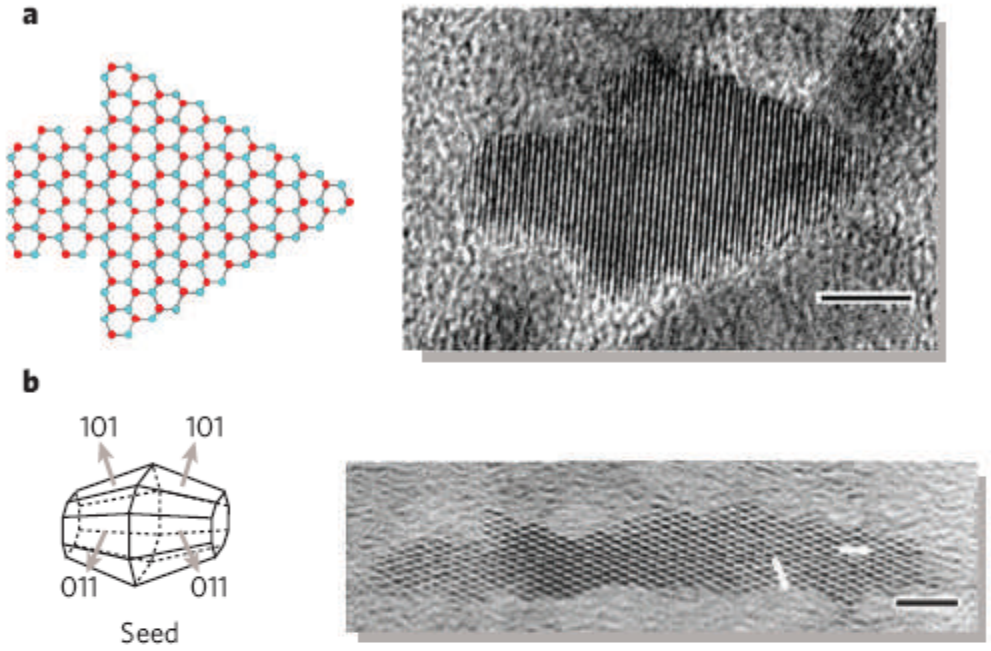

Figure 5 | Nanocrystals with complex shapes prepared by sequential elimination of a high-energy facet. **a**, Two-dimensional representation and a high-resolution TEM image of an arrow-shaped nanocrystal of CdSe. High-resolution TEM characterization shows that each shape of nanocrystal is predominantly wurtzite and that the angled facets of the arrows are the (101) faces. Scale bar, 5 nm. Red and blue dots represent selenium and cadmium atoms, respectively. Reprinted with permission from ref. 22. **b**, Simulated three-dimensional shape and high-resolution TEM analysis of a TiO_2 rod. The long axes of the nanocrystals are parallel to the *c*-axis of the anatase structure, while the nanocrystals are faceted with (101) faces along the short axes. Hexagon shapes (the [010] projection of a truncated octagonal bipyramid) truncated with two (001) and four (101) faces are observed either at the one end or at the centre of the nanocrystals. Scale bar, 3 nm. Reprinted with permission from ref. 35. Copyright (2003) American Chemical Society.

Free boundaries at the micro scale: semiconductors.

Mock (1972), Markowitch (1986), Friedman (1988), Markowich, Ringofer, Schmeiser (1990), Díaz, Galiano, Jüngel (1999), ...

In solid state physics, the drift-diffusion equations are today the most widely used model to describe semiconductor devices. The drift-diffusion models describe the flow of electrons in the conduction band of the semiconductor material and of holes (or defect electrons) in the valence band of the crystal, influenced by the electric field. Mathematically, they form a system of parabolic equations for the electron density n and the hole density p and the Poisson equation for the electric potential V:

$$\frac{\partial n}{\partial t} - \nabla \cdot (\nabla r(n) - n\nabla V) = -R(n, p),$$

$$\frac{\partial p}{\partial t} - \nabla \cdot (\nabla r(p) + p\nabla V) = -R(n, p),$$

$$\Delta V = n - p - C(x) \quad \text{in } Q_T = \Omega \times (0, T),$$

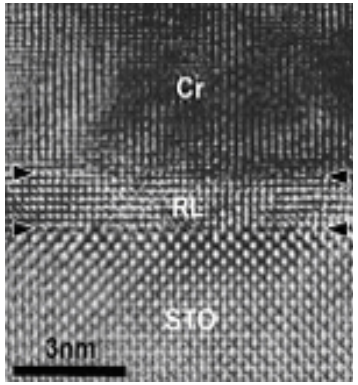

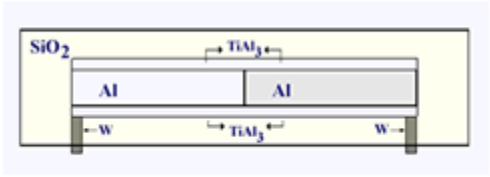

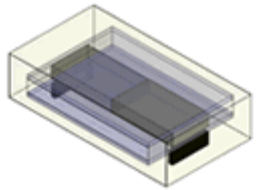

Different point of view:

Is it possible to show (rigourously) the existence of some free boundary arising at the macroscopic scale but not arising at the microscopic scale?

Some similar philosophy (but not exactly the same) in many other contexts:

Approximate problem (without free boundary) / Límit problem (with a free boundary)

- Obstacle problem (Approximate problem = penalisation)
- Cavitation in hidrodynamic lubrication (Approximate problem = aproximation of the Heaviside function)
- Porous media equation and/or NonNewtonian flows (Approximate problem = uniformly parabolic equations)

Question: the scale as an approximating argument ?

Plan:

2.2. A model problem arising in Chemical Engineering and a mathematical tool: homogenization.

2.3. Model problem: effective chemical reactions. Convergence.

2.4. Macroscopic “dead core” versus microscopic strictly positive solutions.

2.5. An isoperimetric inequality for the (macroscopic) dead core.

2.6. Effectiveness as cost fonctional in optimal and controllability shape design problems.

2. 2. A model problem arising in Chemical Engineering and a mathematical tool: homogenization.

Incompressible flow of a fluid reacting with the exterior of many packed solid particles: Absorption and adsorption phenomena in beds or towers. Of relevance in Chemical Engineering (separation, chemical industry, etc).

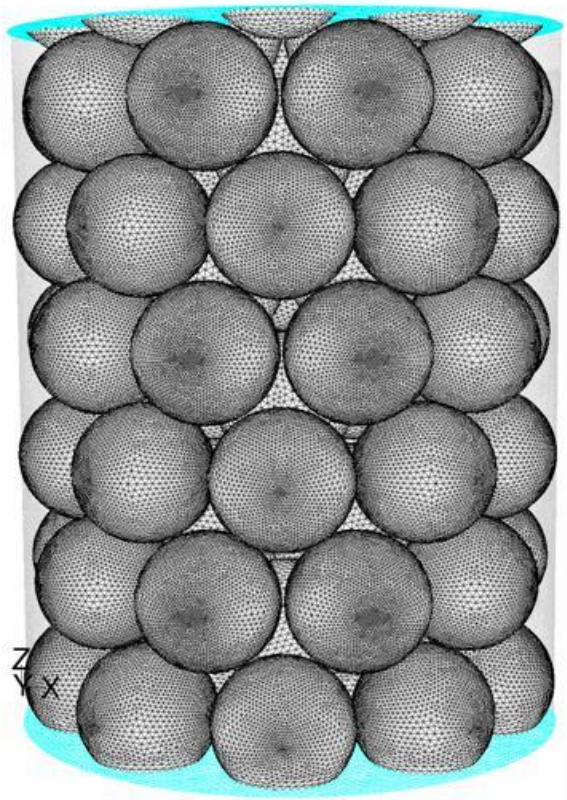

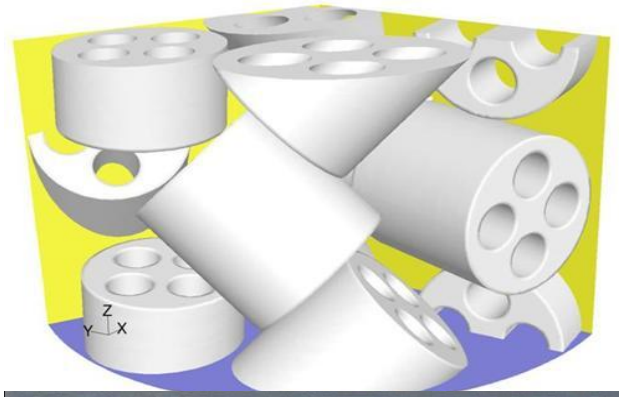

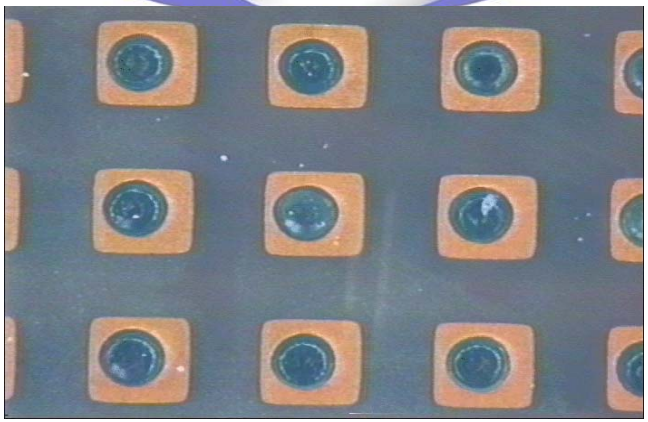

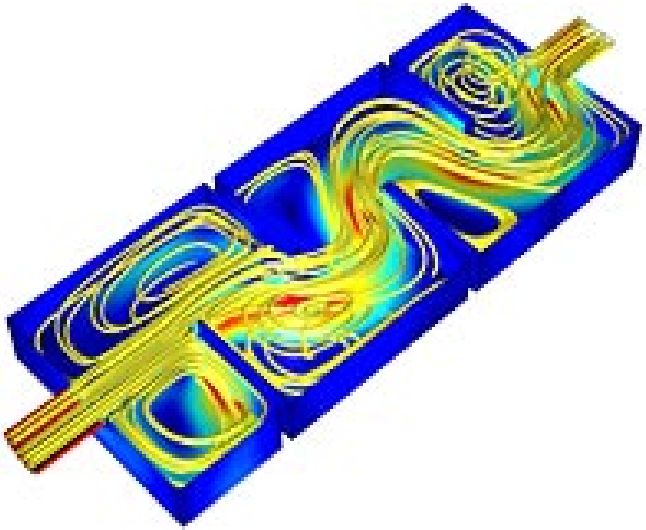

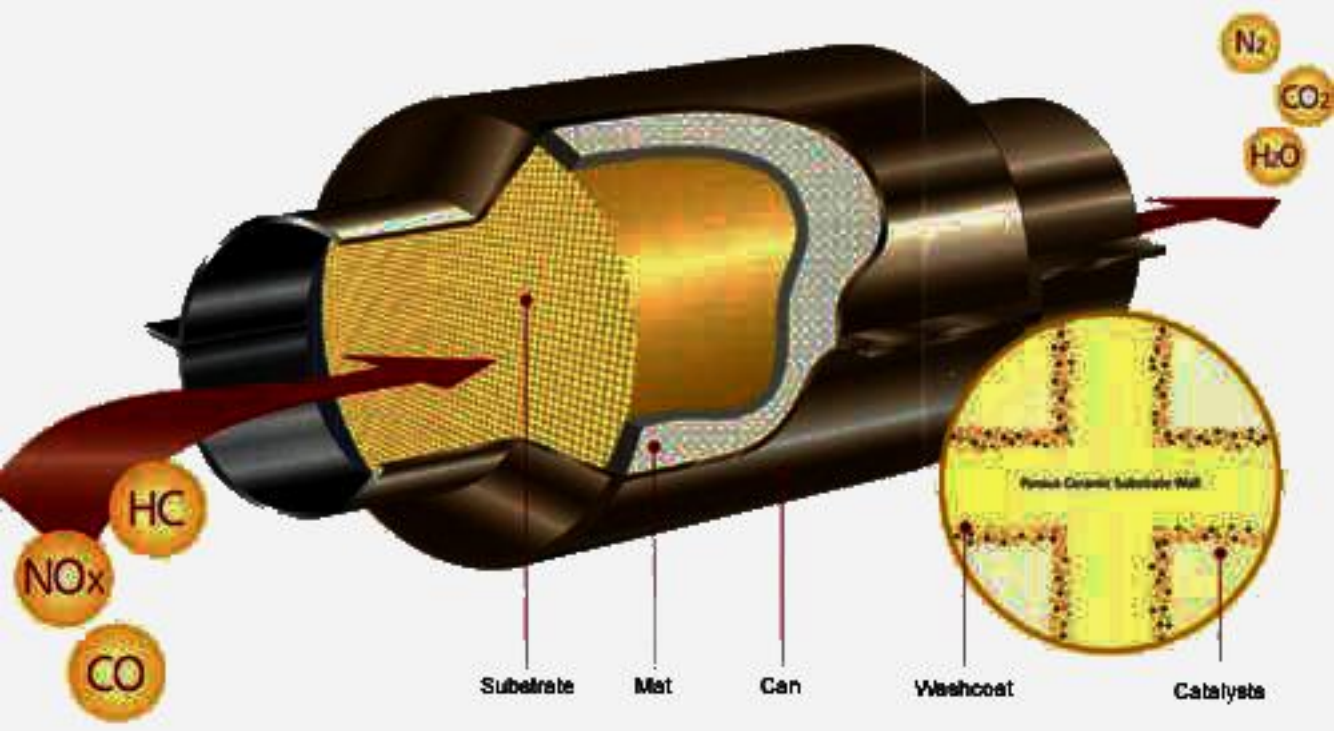
N2
CO2
H2O
HC
NOx
CO
Substrate
Mat
Can
Washcoat
Catalysts

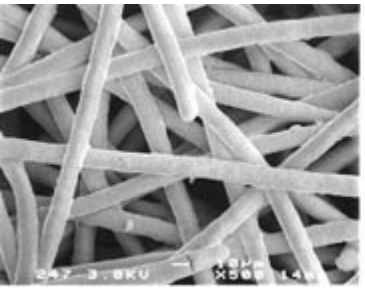

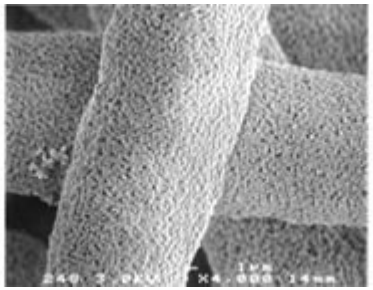

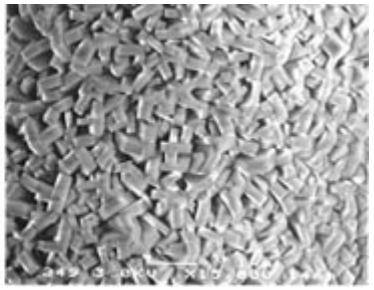

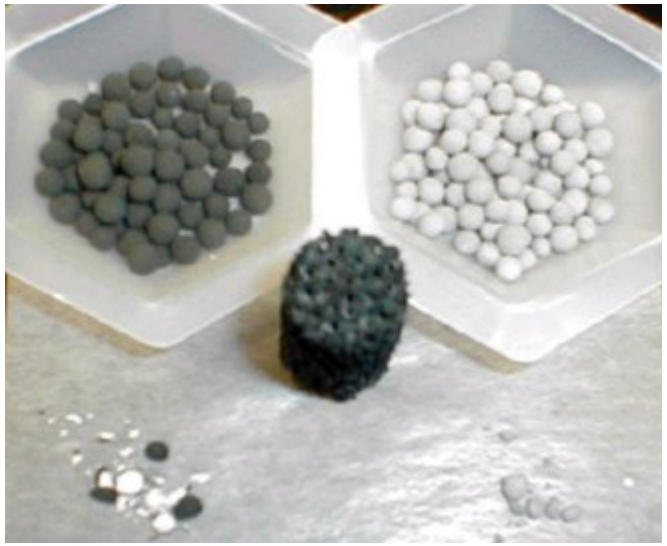

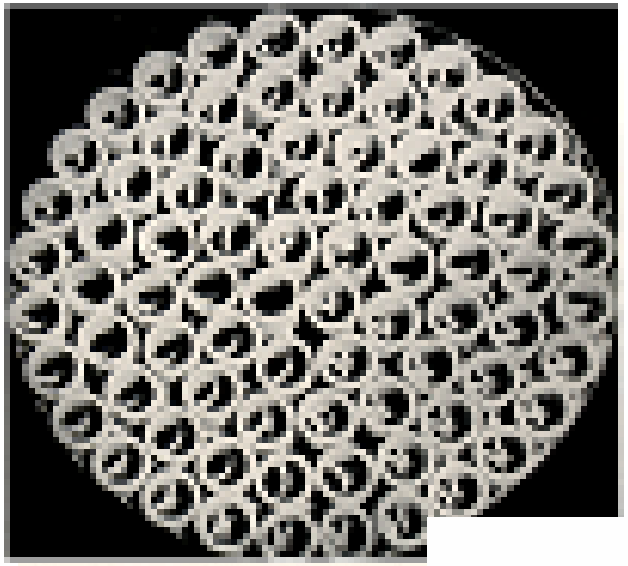

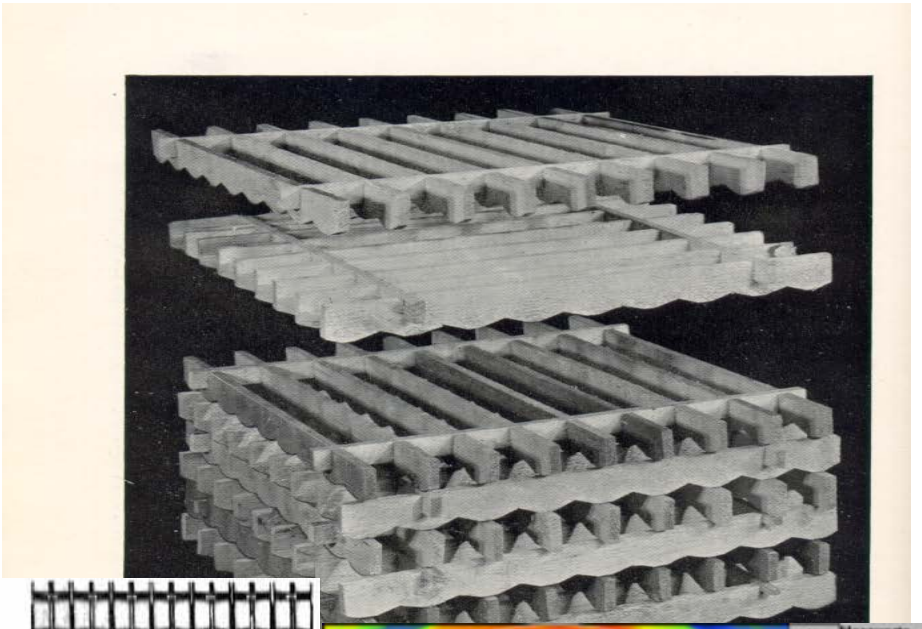

Equipo para contacto de fase múltiple

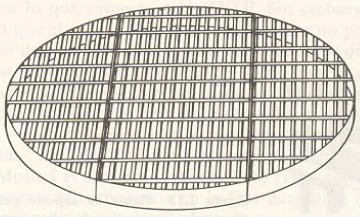

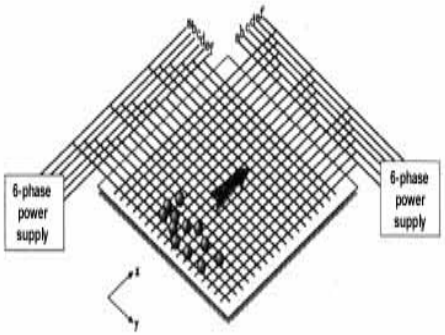

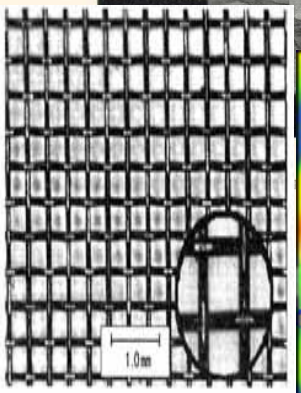

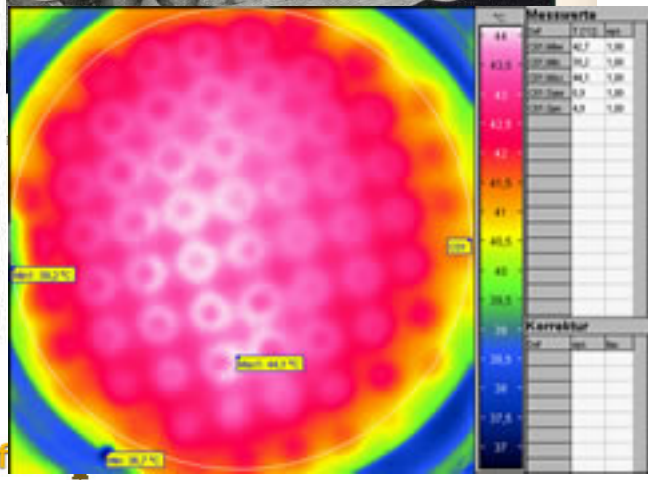

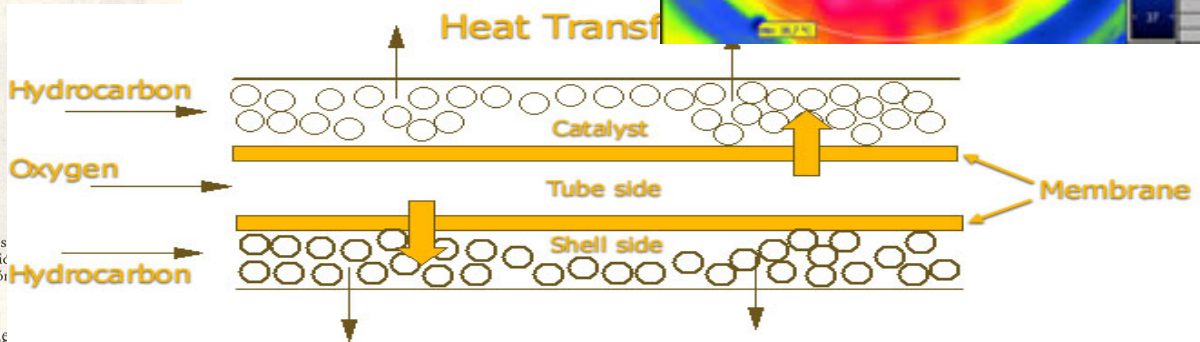

Figura 2.11 Platos
(*a*) Plato de retenci
(*c*) Plato de sujeció
Engineering Co.)

quido se crea por combinación de los efectos de penetración de

Homogenization: process related to the overall modelling in presence of a double spatial scale

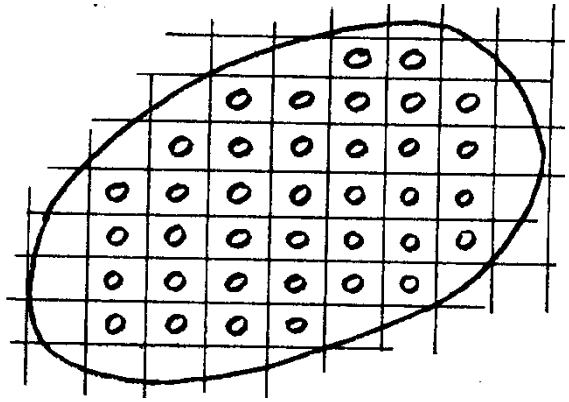

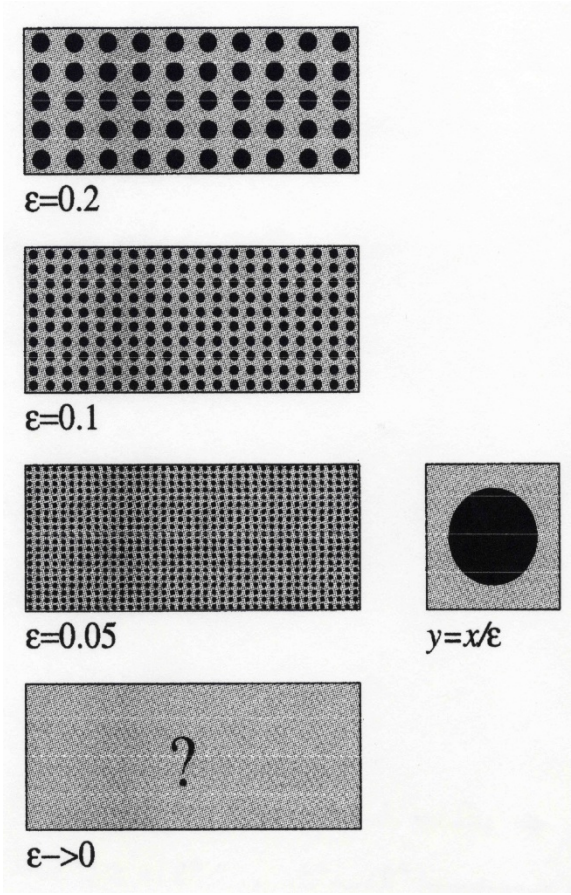

Sánchez-Palencia, Bensoussan-Lions-Papanicolau,...

Many availible convergence methods, variants, applications, …

In general, if u is a "physical magnitud" defined on Ω_ε

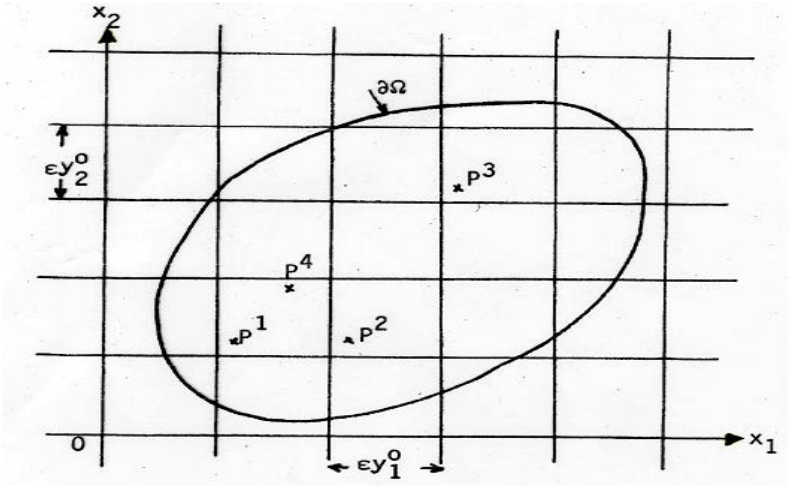

If P_1, P_2 periodically homologous and not far in the $x-$scale then $u(P_1) \approx u(P_2)$.

If P_3 is periodically homologous to P_1, P_2 but far in the $x-$scale then $u(P_1) \approx u(P_3)$ but $u(P_1) \not\approx u(P_3)$.

If P_4 is far (in the $y-$scale) from P_1 (and P_2) but near in the $x-$scale then $u(P_1) \not\approx u(P_3)$ but $u(P_1) \approx u(P_3)$.

$$u^\varepsilon = u^\varepsilon(x) = u^\varepsilon(x,y) \mid_{y=\frac{x}{\varepsilon}}$$

• **Homogeneization**: Question: $u^\varepsilon \to ?$, as $\varepsilon \to 0$ (homogeneized region Ω)

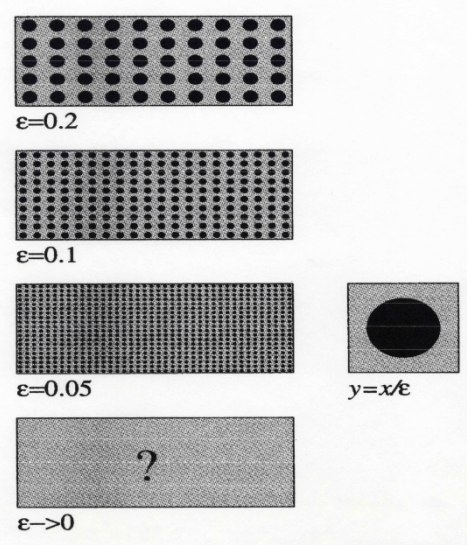

•Two different steps:

a. *Formal Asymptotic Expansion.* "Ansatz"

$$u^\varepsilon(x) = u^\varepsilon(x,y)\,|_{y=\frac{x}{\varepsilon}} = u_0(x,y) + \varepsilon u_1\ (x,y) + \varepsilon^2 u_2(x,y) +$$

with

$u_i\ (x,y)$ Y-periodic with respect to the $y = \dfrac{x}{\varepsilon}$ variable.

Then $u^\varepsilon \to u_0$, as $\varepsilon \to 0$.

b. *Rigurous proof.* There exists a u_0 such that $u^\varepsilon \to u_0$, in some functional space, as $\varepsilon \to 0$.

2. 3. Model problem: effective chemical reactions. Convergence.

C. Conca, J.I. Díaz, A. Liñan and C. Timofte, Homogenization in Chemical Reactive Flows through Porous Media, *Electr. J. Diff. Eqns.* 2004, 1-22.

The stationary reactive flow of a fluid confined in Ω^ε, of concentration u^ε, reacting on the boundary of the catalytic particles (obstacles)

$$\begin{cases} -D_f \Delta u^\varepsilon = f & \text{in } \Omega^\varepsilon, \\ -D_f \dfrac{\partial u^\varepsilon}{\partial \nu} = a\varepsilon g(u^\varepsilon) & \text{on } S^\varepsilon, \\ u^\varepsilon = 0 & \text{on } \partial\Omega. \end{cases}$$

$$g(v) = |v|^{p-1}v, \quad 0 < p < 1 \quad \text{(Freundlich kinetics)}$$

Ω - smooth bounded domain in $\mathbb{R}^n$ $(n \geq 3)$

$Y = [0, l_1[\times ... [0, l_n[$ -the representative cell in $\mathbb{R}^n$

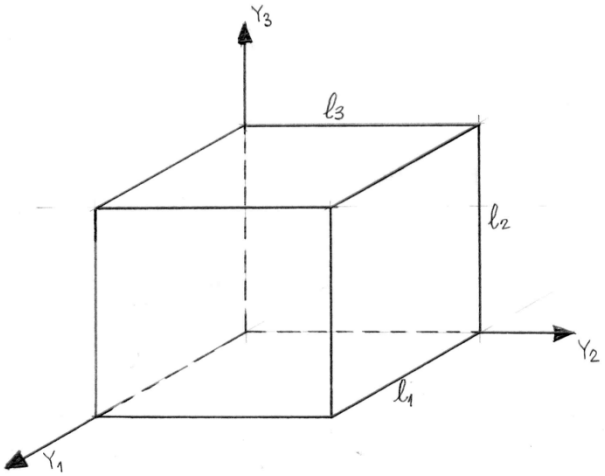

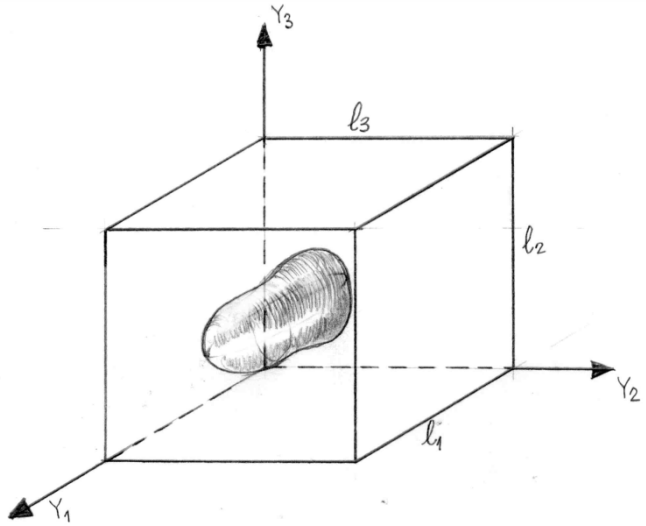

$\overline{T} \subset Y$ - the elementary obstacle $Y^* = Y \setminus \overline{T}, \quad \rho = \dfrac{|Y^*|}{|Y|}.$

T_k^ε -translated image of εT by the vector $(k_1 l_1, ..., k_n l_n)$

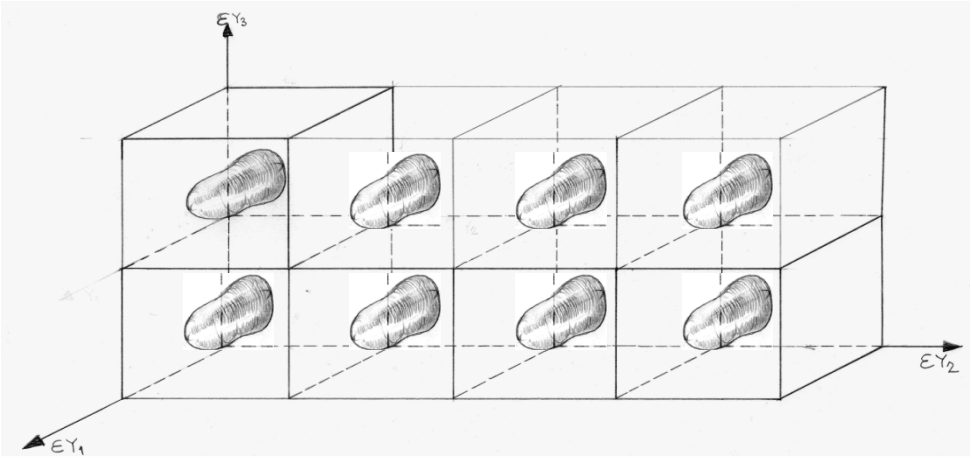

$$T_k^\varepsilon = \varepsilon(kl + T)$$

T^ε the set of all the obstacles contained in Ω, i.e.

$$T^\varepsilon = \bigcup \{ T_k^\varepsilon \mid \overline{T_k^\varepsilon} \subset \Omega,\ k \in Z^n \}.$$

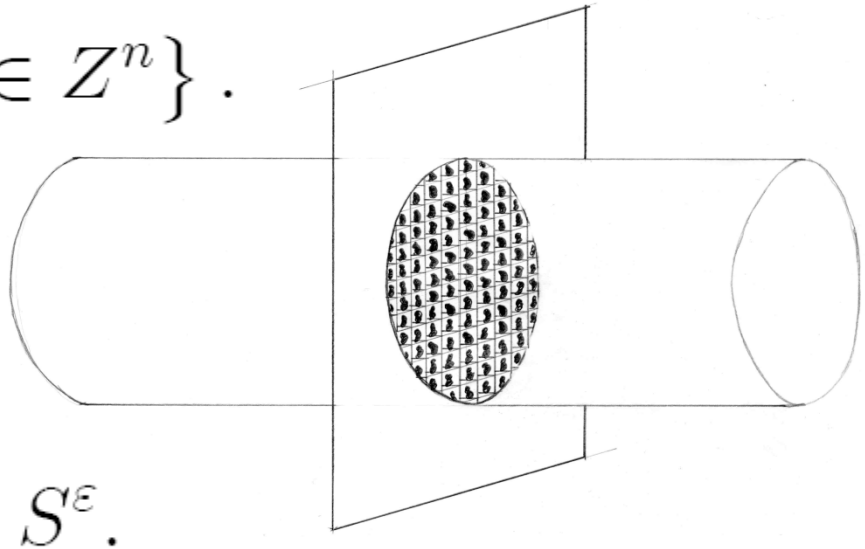

$$\Omega^\varepsilon = \Omega \setminus \overline{T^\varepsilon}, \quad \partial\Omega^\varepsilon = \partial\Omega \cup S^\varepsilon.$$

$$S^\varepsilon = \cup \{ \partial T_k^\varepsilon \mid \overline{T_k^\varepsilon} \subset \Omega,\ k \in Z^n \}.$$

Theorem (CDLT 2004).

Assume $f \in \grave{L}^2(\Omega)$. Then, we can construct an extension $P^\varepsilon u^\varepsilon$ of the solution u^ε such that

$$P^\varepsilon u^\varepsilon \rightharpoonup u \quad \text{weakly in} \quad H_0^1(\Omega)$$

and u is the unique solution of the problem

$$\begin{cases} -\displaystyle\sum_{i,j=1}^{n} q_{ij} \frac{\partial^2 u}{\partial x_i \partial x_j} + a \frac{|\partial T|}{|Y^*|} g(u) = f & \text{in } \Omega, \\ \\ u = 0 & \text{on } \partial\Omega, \end{cases}$$

where $\mathbf{Q} = ((q_{ij}))$ is the "classical homogenized matrix":

$$q_{ij} = D_f \{ \delta_{ij} + \frac{1}{|Y^*|} \int_{Y^*} \frac{\partial \chi_j}{\partial y_i} dy \}$$

with χ_i, $i = 1, ..., n$ solution of the "cell problems"

$$\begin{cases} -\Delta\chi_i = 0 \ \text{ in } \ Y^*, \\ \dfrac{\partial(\chi_i + y_i)}{\partial\nu} = 0 \ \text{ on } \ \partial T, \\ \chi_i \ \ Y- \ \text{ periodic.} \end{cases}$$

The proof uses an energy method applied to weak solutions (Tartar (1978)), a priori estimates and some properties of maximal monotone graphs (Brezis (1973)).

2. 4. Macroscopic “dead core” versus microscopic strictly positive solutions.

In order to study the formation of the interface given by the boundary of the support (the boundary of the “dead core”) we assume

$$f \in L^{\infty}(\Omega) \text{ and } f(x) \geq 0 \text{ , a.e. } x \in \Omega.$$

$$S(f) := \text{ support of } f \subsetneq \Omega$$

Theorem

i) $\forall\ \varepsilon > 0\ \ u^{\varepsilon}(x) > 0$ *in* Ω^{ε} *and so* $S(u^{\varepsilon}) = \Omega^{\varepsilon}$.

ii) For fixed Ω *and* $Y = [0, l_1[\times ...[0, l_n[$ *(the representative cell in* R^n*), there exists a continuous function* $\delta = \delta(\|f\|_{L^{\infty}(\Omega)}, |T|, |\partial T|, \Lambda_0)$*, with* Λ_0 *the larger eigenvalue of the matrix* Q*, i.e. verifying that*

$$\Lambda_0 \left\| \overrightarrow{\xi} \right\|^2 \geq \sum_{i,j=1}^{n} q_{ij}\xi_i\xi_j \quad \text{for any} \quad \overrightarrow{\xi} \in \mathbb{R}^n,$$

such that if δ *is small enough then* $S(u) \subsetneqq \Omega$ *and so* u *gives rise to the free boundary* $F := \partial S(u)$*. Moreover, function* $\delta(\|f\|_{L^{\infty}(\Omega)}, |T|, |\partial T|, \Lambda_0)$ *depends increasingly of* $\|f\|_{L^{\infty}(\Omega)}$ *and decreasingly of* $|T|$, $|\partial T|$ *and* Λ_0.

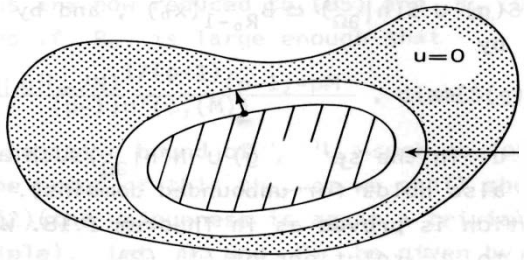

$S(f) :=$ support of f

2. 5. An isoperimetric inequality for the (macroscopic) dead core.

Besides the usual comparison (or maximum) principle we can use another comparison principle of a different nature: the *symmetrized mass comparison principle*.

The process of *symmetrization* applied to problem

$$P(0)\begin{cases} -Lu+\lambda g(u) = f & \text{in } \Omega \\ u = 0 & \text{on } \partial\Omega \end{cases}$$

now for g continuous nondecreasing, $g(0) = 0$ (so that it can be applied to problem $P_0(1)$).

We start by the *symmetrization of the domain* Ω:

Given Ω, an open bounded set of $\mathbb{R}^N$, the symmetrized version of Ω is the ball centered at the origin having the same measure than Ω. Let us call Ω^* to this ball.

Once we know condition $m(\Omega) = m(\Omega^*)$ we can use the *isoperimetric inequality*

$$L \geq N\omega_N^{\frac{1}{N}} A^{\frac{N-1}{N}}$$

where L is the *length* of $\partial\Omega$ (or $m(\partial\Omega)$), A is the *area* of Ω (or $m(\Omega)$) and

ω_N is the *area* of the unit ball of $\mathbb{R}^N$ (i.e. $\omega_N = m(S^{N-1})$)

the equality holds if and only if Ω is a ball.

This was a first noted by Dido de Cartago (850 B.C.) (*in $\mathbb{R}^2$ the circles are the domains with fixed area having smallest perimeter*). Rigorous proofs of (1) are due to Steiner (1882), Schwarz (1890) and Schmidt (1939).

The second step of the process of symmetrization consists in the *symmetrization of data* f and u_0.

We shall use the notion of the *decreasing symmetric rearrangement* of a function introduced by H.A. Schwarz in 1890:

Given a function $h : \Omega \to I\!R$, $h \in L^1(\Omega)$, we define the *decreasing symmetric rearrangement of* h, h^*, as the (unique) function $h^* : \Omega^* \to I\!R$ such that h^* is symmetric (i.e. $h^*(x) = h^*(\widehat{x})$ if $|x| = |\widehat{x}|$), h^* decreases if $|x|$ decreases and the level sets of h and h^* are equimeasurables (i.e. $m(\{x \in \Omega : h(x) > \theta\}) = m(\{x \in \Omega^* : h^*(x) > \theta\}), \forall \theta \in I\!R$).

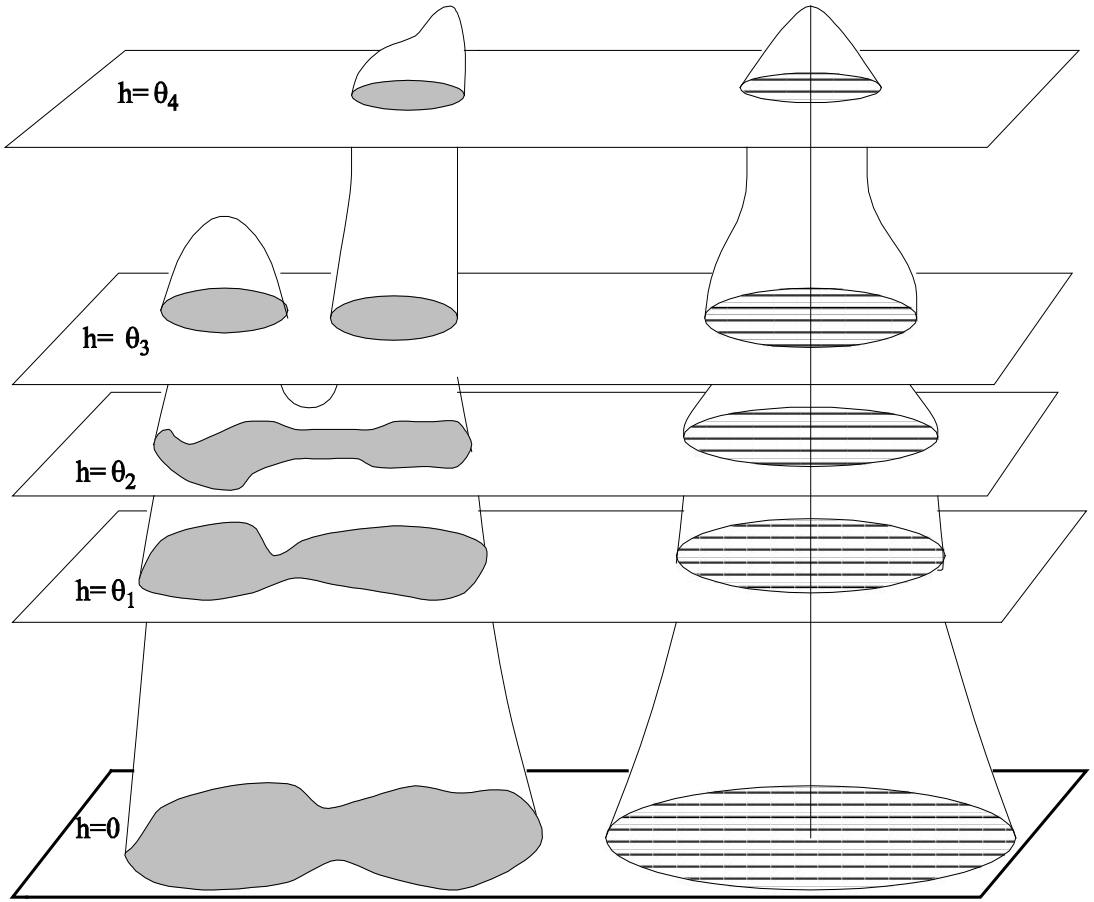

A more systematic definition of h^* can be introduced: we first define the *distribution function of* h by

$$\mu : \mathbb{R} \to \mathbb{R},\ \mu(\theta) := m\{x \in \Omega : h(x) > \theta\}.$$

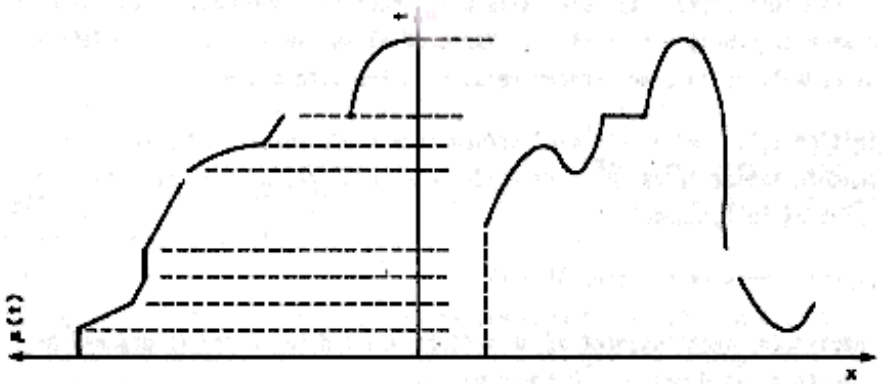

Then we define the *scalar decreasing rearrangement of* h by

$$\widetilde{h} : (0, m(\Omega)] \to \mathbb{R},\ \widetilde{h}(s) := \inf\{\theta \in \mathbb{R} : \mu(\theta) \leq s\}$$

(notice that $\widetilde{h}(s) \sim \mu^{-1}(s)$). Finally, we define the *symmetric decreasing rearrangement of* h, by

$$h^* : \Omega^* \to \mathbb{R},\ h^*(x) := \widetilde{h}(\omega_N |x|^N).$$

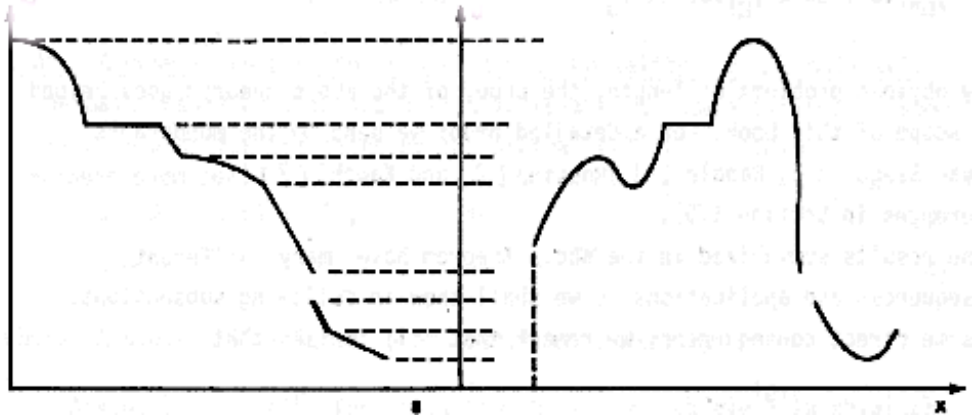

Notice that, since h^* is symmetric, we can write $h^*(x) = H(|x|)$ with $H : \mathbb{R} \to \mathbb{R}$. Nevertheless $H \neq \widetilde{h}$ since $H(r) = \widetilde{h}(\omega_N r^N)$. Notice, also, that assumed $h \geq 0$, by construction, we have that

$$h \in L^1(\Omega) \text{ implies that } h^* \in L^1(\Omega^*) \text{ and}$$

$$\int_\Omega h(x)dx = \int_{\Omega^*} h^*(x)dx \ (\textit{the Cavalieri Principle})$$

and that

$$h \in L^\infty(\Omega) \text{ implies that } h^* \in L^\infty(\Omega^*) \text{ and}$$

$$\operatorname*{esssup}_{x\in\Omega} h(x) = \operatorname*{esssup}_{x\in\Omega^*} h^*(x).$$

The third step of the process is the *symmetrization of the second order operator.*

We must replace the diffusion operator

$$Lu = \sum_{i,j=1}^{N} \frac{\partial}{\partial x_i}(q_{ij}\frac{\partial u}{\partial x_j})$$

by another *isotropic* diffusion operator, i.e. with the same behavior in any direction x_i.

Once we know that Lu is an elliptic operator

$$\sum_{i,j=1}^{N} q_{ij}\xi_i\xi_j \geq \alpha \left\| \overrightarrow{\xi} \right\|^2 \text{ for any } \overrightarrow{\xi} \in \mathbb{R}^N, \text{ for some } \alpha > 0.$$

Then we define *as symmetrized operator of* Lu the one given by

$$L^*u = \alpha \Delta u$$

Summarizing, we say that the *symmetrized problem of* (P) is the following one:

Problem $P^*(0)$: Find $U : \Omega^* \to I\!R$ such that

$$P^*(0) \begin{cases} -\alpha \Delta U + \lambda g(U) = f^*(x), & x \in \Omega^*, \\ U = 0, & x \in \partial\Omega^*. \end{cases}$$

Here $f^*(\cdot)$ is the decreasing symmetric rearrangement of $f(\cdot)$.

Some remarks on the statement of the *symmetrized mass comparison principle.*

The first one is that some pioneer authors finding different relations between u and U where Saint-Venant (1856), Poya and Szego (1951) and Weimberger (1962). The inequality

$$u^*(x) \leq U(x) \ , \ x \in \Omega^* \tag{2}$$

was first proved by G. Talenti, in 1976, for the case without absorption term $g \equiv 0$.

Unfortunately, this (pointwise) comparison *fails* to be true in presence of absorption terms ($g \neq 0$).

In those cases we only can compare the *distribution of the mass* of u and U

Theorem (Symmetrized Mass Comparison Principle (SMCP))

$$\int_{B(0,r)} g(u(x))^* dx \leq \int_{B(0,r)} g(U(x))dx, \forall r \in [0, R],$$

assumed that $\Omega^* = B(0, R)$.

Notice that this comparison (..., Vázquez (1982),...) can be, equivalently, expressed in terms of scalar decreasing rearrangement as

$$\int_0^s g(\widetilde{u}(\sigma))d\sigma \leq \int_0^s g(\widetilde{U}(\sigma))d\sigma, \ \forall s \in [0, m(\Omega)].$$

The SMCP has many applications (as we shall see). The main philosophy of the applications is that function U can be easily estimated in many cases and thus, thanks to the SMCP, properties for U can be extended in similar properties for u. Some books dealing with the symmetrization process are the ones by Bandle (1980), Mossino (1984), Kawohl (1985) and Díaz (1985).

Corollary *Among all the domains of given volume the volume of the dead core (for problem $P(1)$) is biggest for the sphere*

Several proofs in the literature: Bandle-Sperb-Stakgold (1984) for u analytic, ..., Díaz (1985) by using a very old result by Hardy, Littlewood and Polya (1929).

The sphere is the worst of the cases.

In fact, in Chemical Engineering the "effectiveness" of the reaction is represented by the positive number

$$\eta := \frac{1}{m(\Omega)} \int_\Omega g(u(x))dx$$

u solution of $P(1)$.

As consequence of the *Symmetrized Mass Comparison Principle (SMCP)* we get

Theorem *Let η^* be the effectiveness corresponding to problem $P^*(1)$. Then*

$$\eta^* \leq \eta.$$

Remark. Symmetrization in a partial set of spatial variables (of relevance for transport terms): A. Alvino, G. Trombetti, J. I. Díaz, P. L. Lions. Steiner Symmetrization and Elliptic Equations. *Communications on Pure and Applied Mathematics*, Vol. XLIX, 217-236, 1996.

2. 6. Effectiveness as cost fonctional in optimal and controllability shape design problems.

Given an open set D, with $m(D) > V$, the optimal control problem (with the constraint $m(\Omega) = V$) associated to the cost functional

$$\eta_\Omega = \int_D \frac{g(u_\Omega(x))}{m(\Omega)} dx.$$

Notice that we extended $u_\Omega(x)$ to D by making $u_\Omega(x) = 0$ on $D - \Omega$. Once we prescribe $V = m(\Omega)$ its is possible to find optimal shapes for the

Theorem *Given an open set D, with $m(D) > V$, there exists a domain Ω (the optimal shape) solution of the optimal control problem*

$$Max_{\substack{\Omega \subset D \\ m(\Omega)=V}} \eta_\Omega.$$

The proof uses that $-\eta_\Omega$ is monotone decreasing with respect to inclusions (use the comparison principle) and $\gamma-$lower semicontinuous (Bucur and Buttazzo: *Variational Methods in Some Shape Optimization Problems*, SNS Pisa, 2002, Chapter 5).

Remark *If, for instance D is a ball of $\mathbb{R}^2$, the optimal shape (biggest effectiveness) is of the following type:*

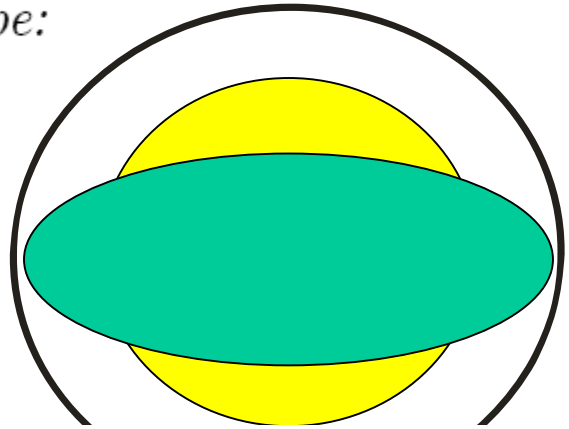

Let us prove now that, for any fixed $\lambda > 0$, there is always a domain Ω of given volume V such that the dead core $N(u)$ is empty. Moreover, there exists a sequence of domains Ω_k such that

$$m(\Omega_k) = V \text{ and } \lim_{k\to\infty} \eta_{\Omega_k} = 1$$

(*approximate controllability* in the J.-L. Lions sense).

We start by an auxiliary result

Lemma *Let w be the solution of $P_0(1)$. Then, if $\psi(x)$ is the (unique) solution of the problem*

$$\begin{cases} -L\psi = 1 & \text{in } \Omega \\ \psi = 0 & \text{on } \partial\Omega \end{cases}$$

we have that $w(x) \leq \psi(x)$ a.e. $x \in \Omega$.

Remark *If $N = 2$ and $L = \Delta$, function ψ coincides (up to a constant factor) with the warping function in the torsion of a cylindrical beam.*

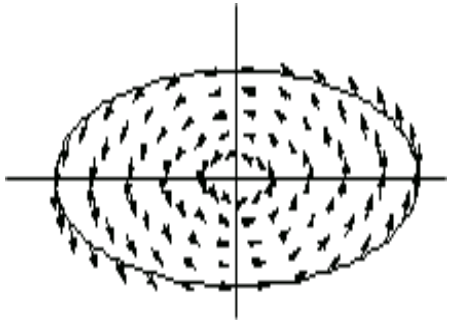

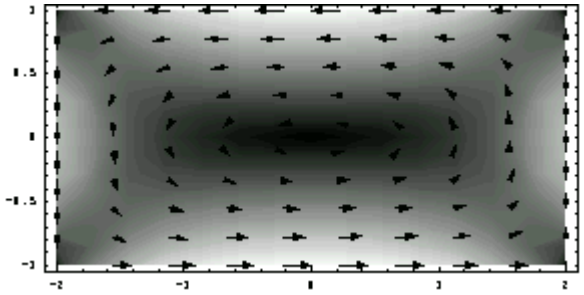

By using rearrangement techniques (C. Bandle, 1985) it was proved that, if L is α-elliptic, then $\|\psi\|^{1+N/2}_{L^\infty(\Omega)} \leq \frac{2+N}{2\alpha\omega_N}(2N)^{-N/2}\|\psi\|_{L^1(\Omega)}$ *and that if λ_1 is the first eigenvalue*

$$\begin{cases} -\Delta\varphi_1 = \lambda_1\varphi_1 & \text{in } \Omega \\ \varphi_1 = 0 & \text{on } \partial\Omega \end{cases}$$

we get $\|\psi\|_{L^1(\Omega)} \leq \frac{V}{\alpha\lambda_1}$ *and thus*

$$\|\psi\|^{1+N/2}_{L^\infty(\Omega)} \leq \frac{2+N}{2\alpha^2\omega_N}(2N)^{-N/2}\frac{V}{\lambda_1}$$

Notice that the well-known Rayleigh-Faber-Krahn inequality

$$\lambda_1(\Omega) \geq (\frac{\omega_N}{V})^{2/N} j_{(N-2)/2}$$

(j_k the first zero of the Bessel function J_k) is not of great use for our purpose.

We must restrict ourselves to "thin" domains and made explicit some lower bounds for λ_1.

We introduce some classes of domains

$$\mathcal{P} = \{\Omega \subset \mathbb{R}^N \text{ lying between two parallel } (N-1)\text{- dimensional hyperplane at distance } 2\rho, \text{ that is all domains of breadth } \leq 2\rho\},$$

$$\mathcal{C}_N = \{\Omega \subset \mathbb{R}^N \text{ convex of inradius } \rho\}$$

Then, we have (Courant-Hilbert, 1924)

$$\lambda_1(\Omega) \geq (\frac{\pi}{2\rho})^2 \text{ for } \Omega \in \mathcal{P},$$

and (Osserman, 1979)

$$\lambda_1(\Omega) \geq (\frac{1}{2\rho})^2 \text{ for } \Omega \in \mathcal{C}_N.$$

By applying the auxiliary lemma and the above inequalities we arrive to

Theorem *Let Ω belong to either $\mathcal{P}$ or $\mathcal{C}_N$. Then there exists $\rho_0 = \rho_0(\alpha, \lambda, N, V)$ such that meas $N(u) = 0$.*

Moreover, given $\varepsilon > 0$ there exists an open set Ω belonging to either $\mathcal{P}$ or $\mathcal{C}_N$, with $m(\Omega) = V$ and such that

$$\eta_\Omega \geq 1 - \varepsilon.$$

A different study can be made by using the microscale data.

*separation among the holes

*size and shape of the obstacles

Many variants are possible:

Microscopic Signorini boundary conditions, Reactions at the interior of the cell, quasilinear equations, …, systems (fluid transport terms), …

Evolution problem (coupled with an ODE)

Controlling the macroscopic behavior by acting at the microscopic scale

Think **globally** and **act locally**

Plan of Section 3:

3.1. The role of a small curvature in the transversal direction a slender or shell.

3.2. Tensegrity structures.

3.1. The role of a small curvature in the transversal direction a slender or shell.

3.1.1. Introduction.

Researches made in a joint paper (*Asymptotic Analysis*, 2007) with **E. Sanchez-Palencia.**

The experience shows that when considering a slender or shell a small curvature in the transversal direction to the main length supply an extra rigidification with respect to the planar case:

* flexible steel retractable meter tape measure, …,

We shall carry out the study of the asymptotic modelling of such kind of shell structures

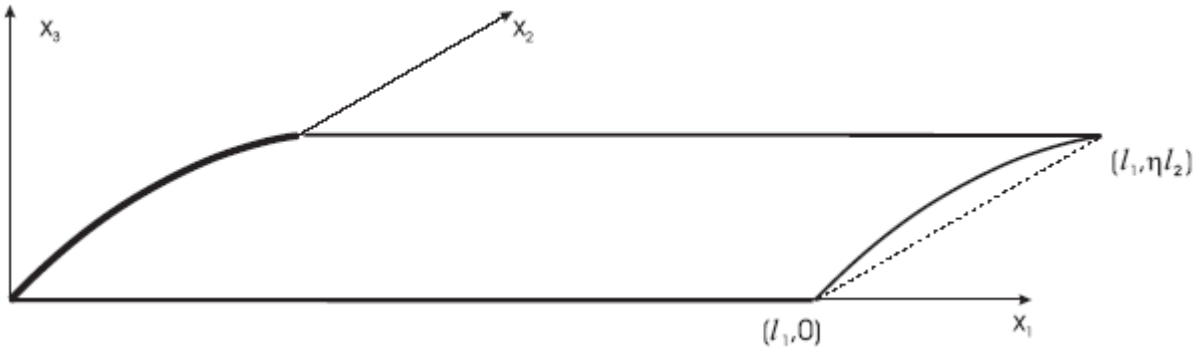

We also will consider more sophisticated structures formed by coupling two of such basic shells by means of an edge with slight folding

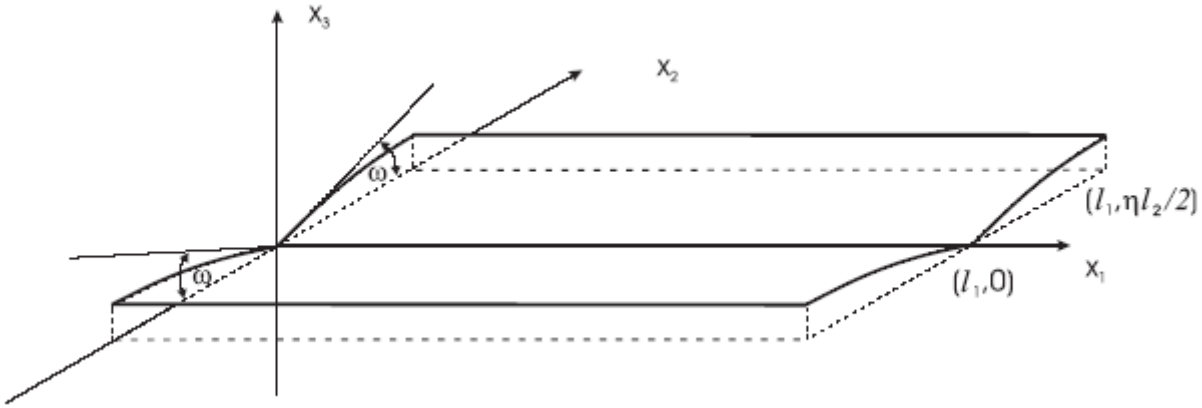

as well as the case of an infinity set of shells obtained by the periodic repetition of the basic structure

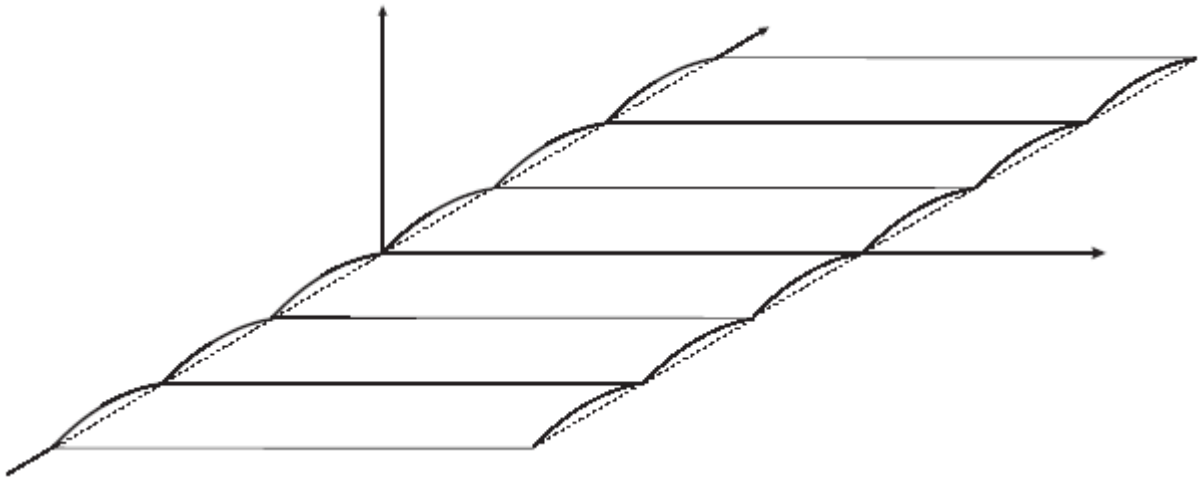

3.2. 2. The basic problem.

We consider a slender cylindrical shell

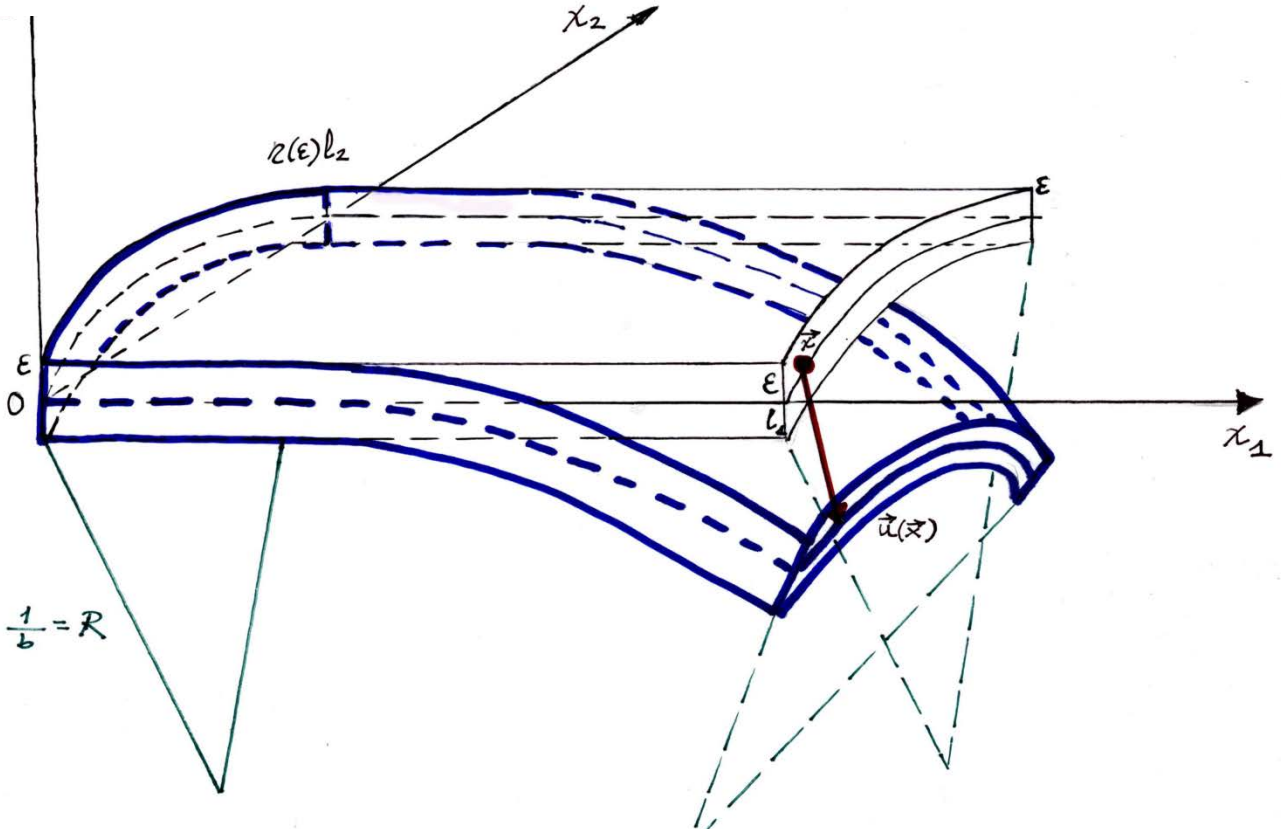

According to standard notations in cylindrical shell theory the "plane of parameters x_1, x_2" is merely the middle surface (cylinder) of the shell developed into a plane. We chose x_1 in the direction of the generators and x_2 normal to them, so that the principal curvatures are zero in the direction x_1 and $b = 1/R$ in the direction x_2, where R denotes the radius of the cross section

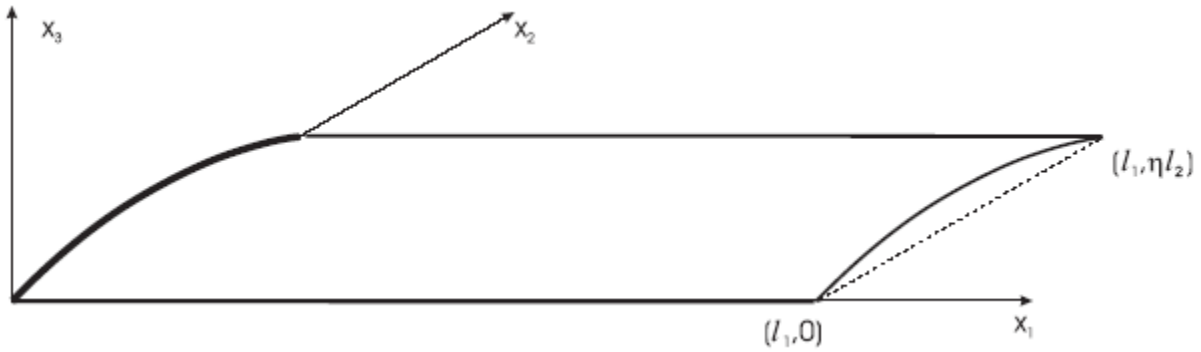

Accordingly, the second fundamental form of the surface has components $b_{11} = b_{12} = 0$ and $b_{22} = b$, Moreover, the Christoffel symbols of the surface vanish identically, so that covariant and classical differentiation coincide. Since $b_{12}^2 - b_{11}b_{22} = 0$ the surface is parabolic, i.e. the directions of the principal curvatures coincide

Let ε be a small parameter, the relative thickness of the plate. Let $\eta = \eta(\varepsilon)$ be a new small parameter satisfying

$$\varepsilon^{1/3} \leq \eta \leq 1.$$

the typical example will be $\eta = \varepsilon^{1/4}$, Let us denote the shell domain by $\Omega_\varepsilon = (0, l_1) \times (0, \eta l_2)$, with $\eta l_2 \leq 2R$.

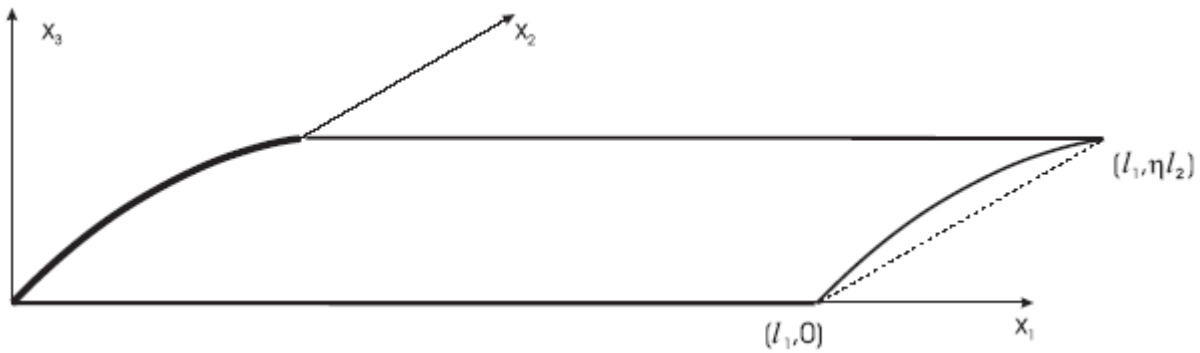

The corresponding tangential displacements are $\tilde{u}_1, \tilde{u}_2$, whereas $\tilde{u}_3$ is the displacement normal to the shell. Some times we shall use the notation $\tilde{\mathbf{u}} = \tilde{\mathbf{u}}^\varepsilon$ to indicate explicitly the ε-dependence.

We shall admit, in this section, that the shell is clamped by the "small curved boundary" $(\{0\} \times [0, \eta l_2]$ and free by the rest This implies the kinematic boundary conditions:

$$0 = \tilde{u}_1 = \tilde{u}_2 = \tilde{u}_3 = \tilde{\partial}_1 \tilde{u}_3 \quad \text{on } \{0\} \times [0, \eta l_2],$$

where

$$\tilde{\partial}_\alpha = \frac{\partial}{\partial x_\alpha}.$$

The space of configuration will be denoted by V_ε. It is the subspace of $H^1(\Omega_\varepsilon) \times H^1(\Omega_\varepsilon) \times H^2(\Omega_\varepsilon)$ formed by the functions satisfying the kinematic boundary conditions

Although it is possible to write the complete system of equations modeling the above elastic problem (the "strong formulation": see. e.g.

F. Niordson, *Shell theory*, North Holland, Amsterdam, 1985

here we shall follow a "variational or weak formulation"

$$\varepsilon a(\mathbf{u}^\varepsilon, \mathbf{v}) + \varepsilon^3 b(\mathbf{u}^\varepsilon, \mathbf{v}) = \langle \mathbf{f}, \mathbf{v} \rangle$$

where the coefficients ε and ε^3 account for the fact that the membrane and flection rigidities are proportional to the thickness of the plate and to its cube, respectively. Moreover, the two bilinear forms $a(\mathbf{u}^\varepsilon, \mathbf{v})$ and $b(\mathbf{u}^\varepsilon, \mathbf{v})$ on the space $\mathbf{V}$ are defined thought the previous expressions (membrane strains in shell theory):

$$\tilde{T}^{\alpha\beta}(\tilde{\mathbf{u}}) = \tilde{T}^{\beta\alpha}(\tilde{\mathbf{u}}) = A^{\alpha\beta\lambda\mu}\tilde{\gamma}_{\lambda\mu}(\tilde{\mathbf{u}})$$

$$\begin{cases} \tilde{\gamma}_{11}(\tilde{\mathbf{v}}) = \tilde{\partial}_1\tilde{v}_1 \\ \tilde{\gamma}_{22}(\tilde{\mathbf{v}}) = \tilde{\partial}_2\tilde{v}_2 + b_3\tilde{v}_3 \\ \tilde{\gamma}_{12}(\tilde{\mathbf{v}}) = \tilde{\gamma}_{21}(\tilde{\mathbf{v}}) = \frac{1}{2}(\tilde{\partial}_2\tilde{v}_1 + \tilde{\partial}_1\tilde{v}_2) \end{cases}$$

and

$$\tilde{\rho}_{\alpha\beta}(\tilde{\mathbf{v}}) = \tilde{\partial}_{\alpha\beta}\tilde{v}_3 \qquad \text{curvature variation tensor}$$

for the triplets $\tilde{\mathbf{v}} = (\tilde{v}_1, \tilde{v}_2, \tilde{v}_3)$.

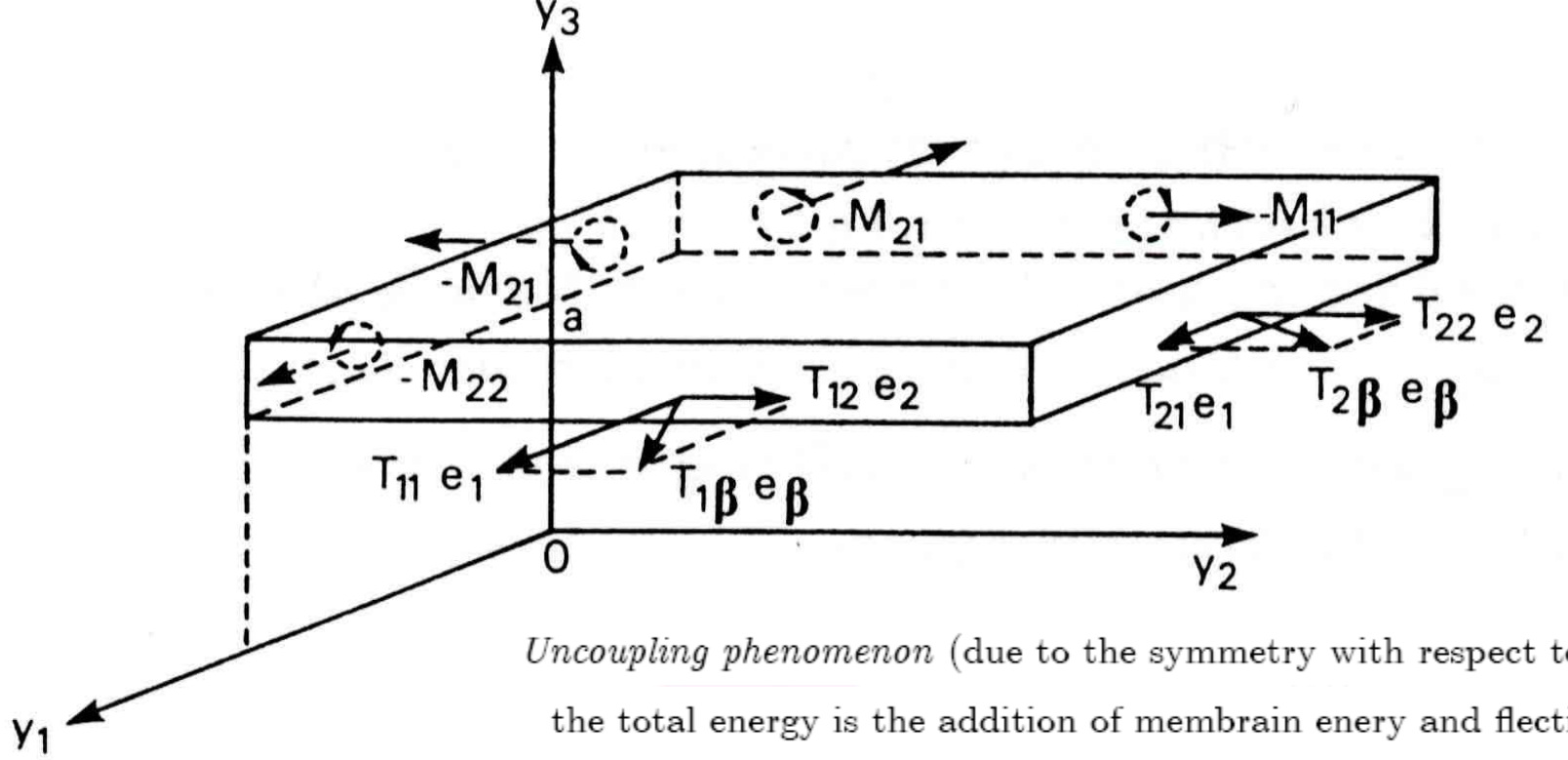

Uncoupling phenomenon (due to the symmetry with respect to $x_3 = 0$):

the total energy is the addition of membrain enery and flection energy

The two bilinear forms on $\mathbf{V}$ are then defined by:

$$a(\tilde{\mathbf{u}}, \tilde{\mathbf{v}}) = \int_{\Omega_\varepsilon} A^{\alpha\beta\lambda\mu} \tilde{\gamma}_{\alpha\beta}(\tilde{\mathbf{u}}) \tilde{\gamma}_{\lambda\mu}(\tilde{\mathbf{v}}) d\mathbf{x}$$

$$b(\tilde{\mathbf{u}}, \tilde{\mathbf{v}}) = \int_{\Omega_\varepsilon} B^{\alpha\beta\lambda\mu} \tilde{\rho}_{\alpha\beta}(\tilde{\mathbf{u}}) \tilde{\rho}_{\alpha\beta}(\tilde{\mathbf{v}}) d\mathbf{x},$$

where the coefficients $A^{\alpha\beta\lambda\mu}$ and $B^{\alpha\beta\lambda\mu}$ satisfy the symmetry and positivity conditions

$$A^{\alpha\beta\lambda\mu} = A^{\beta\alpha\lambda\mu} = A^{\lambda\mu\alpha\beta}$$

$$A^{\alpha\beta\lambda\mu} \theta_{\alpha\beta} \theta_{\lambda\mu} \geq c \theta_{\alpha\beta} \theta_{\alpha\beta} \quad \text{for} \quad \theta_{\alpha\beta} = \theta_{\beta\alpha} \quad \text{with some } c > 0.$$

As applied forces, we shall give a normal loading depending on ε by the factor ε^3

$$\langle \mathbf{f}, \mathbf{v} \rangle = \varepsilon^3 \int_{\Omega_\varepsilon} F_3(x_1, x_2/\eta) \tilde{v}_3(x_1, x_2) d\mathbf{x},$$

We note that the shape of the profile of the applied loading in x_2 is independent of ε but applied to the points x_2/η

We shall admit in the sequel that

$$F_3 \in L^2(\Omega)$$

where

$$\Omega = (0, l_1) \times (0, l_2).$$

Problem P_ε. *Find* $\tilde{\mathbf{u}}^\varepsilon \in \mathbf{V}_\varepsilon$ *satisfying*

$$\varepsilon a(\mathbf{u}^\varepsilon, \mathbf{v}) + \varepsilon^3 b(\mathbf{u}^\varepsilon, \mathbf{v}) = \langle \mathbf{f}, \mathbf{v} \rangle \qquad \forall \tilde{\mathbf{v}} \in \mathbf{V}_\epsilon.$$

Remark

Since the bilinear forms $a(\mathbf{u}, \mathbf{v})$ *and* $b(\mathbf{u}, \mathbf{v})$ *are symmetric, from well known results we deduce that, in fact,* $\tilde{\mathbf{u}}^\varepsilon$ *is the unique solution of the minimization problem*

$$Min_{\mathbf{V}} \widetilde{J}_\varepsilon(\mathbf{v})$$

where

$$\widetilde{J}_\varepsilon(\mathbf{v}) = \frac{\varepsilon}{2} a(\mathbf{v}, \mathbf{v}) + \frac{\varepsilon^3}{2} b(\mathbf{v}, \mathbf{v}) - \langle \mathbf{f}, \mathbf{v} \rangle.$$

The objective of the rest of the section is to study its asymptotic behavior as $\varepsilon \downarrow 0$.

3.1.3. Scaling and a priori estimates in the basic problem.

Let us perform the change of variables :

$$\begin{cases} \mathbf{x} = (x_1, x_2) \Rightarrow \mathbf{y} = (y_1, y_2), \\ y_1 = x_1, \qquad y_2 = \eta^{-1} x_2 \end{cases}$$

so, the domain Ω_ε is transformed into Ω and

$$\partial_1 = \tilde{\partial}_1, \qquad \partial_2 = \eta \tilde{\partial}_2; \qquad \partial_\alpha = \frac{\partial}{\partial y_\alpha}.$$

Moreover, we shall perform the change of unknowns

$$\begin{cases} \tilde{u}_1(\mathbf{x}) = \eta^\theta u_1(\mathbf{y}), \\ \tilde{u}_2(\mathbf{x}) = \eta^{\theta-1} u_2(\mathbf{y}), \\ \tilde{u}_3(\mathbf{x}) = \eta^{\theta-2} b^{-1} u_3(\mathbf{y}), \end{cases}$$

As θ is not defined, the total level of the scaling is not specified, only the mutual ratios of dilatation of the three components are fixed. They are chosen in analogy with layers in parabolic shells. Specifically, the ratio between the components 1 and 2 is fixed in order that the new form of the shear membrane strain $\tilde{e}_{12}$ be formed by two terms of the same order (which, on the other hand, are asymptotically large, forming a constraint for the limit problem). The ratio between the components 2 and 3 is also fixed in such a way that the new form of the membrane strain $\tilde{e}_{22}$ be formed by two terms of the same order.

We then perform the previous change for $\tilde{\mathbf{u}}^\varepsilon$ as well as for $\tilde{\mathbf{v}}$ in P_ε and we have

$$\tilde{\gamma}_{11}(\tilde{\mathbf{v}}) = \eta^\theta \partial_1 v_1$$

$$\tilde{\gamma}_{12}(\tilde{\mathbf{v}}) = \tilde{\gamma}_{21}(\tilde{\mathbf{v}}) = \eta^{\theta-1}\frac{1}{2}(\partial_2 v_1 + \partial_1 v_2),$$

$$\tilde{\gamma}_{22}(\tilde{\mathbf{v}}) = \eta^{\theta-2}(\partial_2 v_2 + v_3),$$

$$\tilde{\rho}_{11}(\tilde{\mathbf{v}}) = \eta^{\theta-2} b^{-1} \partial_1^2 v_3,$$

$$\tilde{\rho}_{12}(\tilde{\mathbf{v}}) = \tilde{\rho}_{21}(\tilde{\mathbf{v}}) = \eta^{\theta-3} b^{-1} \partial_1 \partial_2 v_3, \qquad \tilde{\rho}_{22}(\tilde{\mathbf{v}}) = \eta^{\theta-4} b^{-1} \partial_2^2 v_3.$$

It will prove useful to define

$$\gamma^\varepsilon_{11}(\mathbf{v}) = \partial_1 v_1$$

$$\gamma^\varepsilon_{12}(\mathbf{v}) = \gamma^\varepsilon_{21}(\mathbf{v}) = \eta^{-1}\frac{1}{2}(\partial_2 v_1 + \partial_1 v_2),$$

$$\gamma^\varepsilon_{22}(\mathbf{v}) = \eta^{-2}(\partial_2 v_2 + v_3);$$

$$\rho^\varepsilon_{11}(\mathbf{v}) = \eta^2 \partial_1^2 v_3,$$

$$\rho^\varepsilon_{12}(\mathbf{v}) = \rho_{21}(\mathbf{v}) = \eta \partial_1 \partial_2 v_3,$$

$$\rho^\varepsilon_{22}(\tilde{\mathbf{v}}) = \partial_2^2 v_3.$$

so that:

$$\tilde{\gamma}_{11}(\tilde{\mathbf{v}}) = \eta^\theta \gamma^\varepsilon_{11}(v)$$

$$\tilde{\gamma}_{12}(\tilde{\mathbf{v}}) = \tilde{\gamma}_{21}(\tilde{\mathbf{v}}) = \eta^\theta \gamma^\varepsilon_{12}(\mathbf{v})$$

$$\tilde{\gamma}_{22}(\tilde{\mathbf{v}}) = \eta^\theta \gamma^\varepsilon_{22}(\mathbf{v})$$

$$\tilde{\rho}_{11}(\tilde{\mathbf{v}}) = \eta^{\theta-4} b^{-1} \rho^\varepsilon_{11}(\mathbf{v})$$

$$\tilde{\rho}_{12}(\tilde{\mathbf{v}}) = \tilde{\rho}_{21}(\tilde{\mathbf{v}}) = \eta^{\theta-4} b^{-1} \rho^\varepsilon_{12}(\mathbf{v}) \qquad \tilde{\rho}_{22}(\tilde{\mathbf{v}}) = \eta^{\theta-4} b^{-1} \rho^\varepsilon_2(\mathbf{v}).$$

We recall that the spatial domain is now $\Omega = (0, l_1) \times (0, l_2)$. The space of configuration, after scaling will be denoted by $\mathbf{V}$. It is the subspace of

$$H^1(\Omega) \times H^1(\Omega) \times H^2(\Omega)$$

formed by the functions satisfying the kinematic boundary conditions

$$0 = u_1 = u_2 = u_3 \text{ on } \{0\} \times [0, l_2].$$

The expression $\varepsilon a(\mathbf{u}^\varepsilon, \mathbf{v}) + \varepsilon^3 b(\mathbf{u}^\varepsilon, \mathbf{v}) = \langle \mathbf{f}, \mathbf{v} \rangle$ then becomes:

$$P \int_\Omega A^{\alpha\beta\lambda\mu} \gamma^\varepsilon_{\alpha\beta}(\mathbf{u}_\varepsilon) \gamma^\varepsilon_{\lambda\mu}(\mathbf{v}) d\mathbf{y} + Q \int_\Omega B^{\alpha\beta\lambda\mu} \rho^\varepsilon_{\alpha\beta}(\mathbf{u}^\varepsilon) \rho^\varepsilon_{\lambda\mu}(\mathbf{v}) d\mathbf{y} = R \int_\Omega F_3(y_1, y_2) v_3(y_1, y_2) d\mathbf{y},$$

with

$$P = \varepsilon \eta^{2\theta+1}$$

$$Q = \varepsilon^3 \eta^{2\theta-7} b^{-2}$$

we shall determine the $b(\varepsilon)$ and θ as functions of ε and the function $\eta(\varepsilon)$ using the two equations

$$P = Q = R.$$

This gives $b = \varepsilon/\eta^4$ and $\eta^{\theta-2} = \varepsilon$.

b is always small with respect to η^{-1} , and equal to 1 (or rather 0(1)) in the "typical example" $\eta = \varepsilon^{1/4}$ we have $\theta = 6$.

Once θ is determined, the scaling is perfectly defined. We then observe that the factor $\eta^{\theta-2}b^{-1}$

$$\tilde{u}_3(\mathbf{x}) = \eta^{\theta-2}b^{-1}u_3(\mathbf{y}),$$

takes the form: η^4 which is always small. It means that the scaling of the component u_3^ε is such that, after scaling, it is asymptotically large with respect to the case before scaling. As we shall prove in the sequel, the scaled unknown u_3^ε has a non zero limit; it follows that the initial unknown $\tilde{u}_3^\varepsilon$ tends to 0 at the ratio η^4. We shall come again on this property, which amounts to the rigidification of the plate with respect to the plane case.

Summing up, the problem P_ε becomes after scaling:

Problem Π_ε. *Find* $\mathbf{u}^\varepsilon \in \mathbf{V}$ *satisfying*

$$a^\varepsilon(\mathbf{u}^\varepsilon, \mathbf{v}) = \int_\Omega F_3(y_1, y_2)v_3(y_1, y_2)d\mathbf{y}.$$

$\forall v \in \mathbf{V}$, *where*

$$a^\varepsilon(\mathbf{u}^\varepsilon, \mathbf{v}) \overset{def}{=} \int_\Omega A^{\alpha\beta\lambda\mu}\gamma^\varepsilon_{\alpha\beta}(\mathbf{u}^\varepsilon)\gamma^\varepsilon_{\lambda\mu}(\mathbf{v})d\mathbf{y} + \int_\Omega B^{\alpha\beta\lambda\mu}\rho^\varepsilon_{\alpha\beta}(\mathbf{u}^\varepsilon)\rho^\varepsilon_{\lambda\mu}(\mathbf{v})d\mathbf{y}.$$

It should be emphasized that, by virtue of the definitions the coefficients involve various powers of η, running from -4 to $+4$. The terms in η^{-4} to η^{-1} are "penalty terms", whereas those in η^1 to η^4 are "singular perturbation terms". Only the terms of order 1 will remain in the limit expression.

Remark $\mathbf{u}^\varepsilon$ *is the unique solution of the minimization problem*

$$Min_{\mathbf{V}} J_\varepsilon(\mathbf{v})$$

where

$$J_\varepsilon(\mathbf{v}) = \frac{1}{2}a^\varepsilon(\mathbf{v}, \mathbf{v}) - \langle \mathbf{f}, \mathbf{v} \rangle.$$

Let us proceed to the a priori estimates. From the expression of $a^\varepsilon(\mathbf{v},\mathbf{v})$ with $\mathbf{u}^\varepsilon = \mathbf{v}$,

Lemma *The estimates:*

$$\|\partial_1 v_1\|^2_{L^2(\Omega)} \le c a^\varepsilon(\mathbf{v},\mathbf{v})$$

$$\|\eta^{-1}\frac{1}{2}(\partial_2 v_1 + \partial_1 v_2)\|^2_{L^2(\Omega)} \le c a^\varepsilon(\mathbf{v},\mathbf{v})$$

$$\|\eta^{-2}(\partial_2 v_2 + v_3)\|^2_{L^2(\Omega)} \le c a^\varepsilon(\mathbf{v},\mathbf{v})$$

$$\|\partial_2^2 v_3\|^2_{L^2(\Omega)} \le c a^\varepsilon(\mathbf{v},\mathbf{v})$$

$$\|\eta\partial_1\partial_2 v_3\|^2_{L^2(\Omega)} \le c a^\varepsilon(\mathbf{v},\mathbf{v})$$

$$\|\eta^2\partial_1^2 v_3\|^2_{L^2(\Omega)} \le c a^\varepsilon(\mathbf{v},\mathbf{v})$$

hold true for a certain $c > 0$ independent of ε and $\mathbf{v} \in \mathbf{V}$.

Now, in order to prove that the functional in the right hand side is bounded independently of ε, we need an estimate on u_3 itself.

Lemma *The estimate:*

$$\|v_3\|^2_{L^2((0,l_1);H^2(0,l_2))} \le c a^\varepsilon(\mathbf{v},\mathbf{v})$$

holds true for a certain $c > 0$ independent of ε and $\mathbf{v} \in \mathbf{V}$.

PROOF. Discarding the factors in η and differentiating we have:

$$\|\partial_2^2 v_1 + \partial_2\partial_1 v_2)\|^2_{L^2((0,l_1);H^{-1}(0,l_2))} \le c a^\varepsilon(\mathbf{v},\mathbf{v})$$

$$\|\partial_1\partial_2 v_2 + \partial_1 v_3)\|^2_{H^{-1}((0,l_1);L^2(0,l_2))} \le c a^\varepsilon(\mathbf{v},\mathbf{v}).$$

using the fact that v_1 vanishes on $\{0\} \times [0, l_2]$, by using the Poincaré's inequality we obtain:

$$\|v_1\|^2_{H^1((0,l_1);L^2(0,l_2))} \leq ca^\varepsilon(\mathbf{v}, \mathbf{v})$$

and differentiating,

$$\|\partial_2^2 v_1\|^2_{H^1((0,l_1);H^{-2}(0,l_2)))} \leq ca^\varepsilon(\mathbf{v}, \mathbf{v}).$$

taking the weaker norm, it follows that

$$\|\partial_2 \partial_1 v_2\|^2_{L^2((0,l_1);H^{-2}(0,l_2))} \leq ca^\varepsilon(\mathbf{v}, \mathbf{v})$$
$$\|\partial_1 v_3\|^2_{H^{-1}((0,l_1);H^{-2}(0,l_2))} \leq ca^\varepsilon(\mathbf{v}, \mathbf{v})$$

or even (integrating with respect to y_1 on account of the vanishing of the trace on $\{0\} \times [0, l_2]$):

$$\|v_3\|^2_{L^2((0,l_1);H^{-2}(0,l_2))} \leq ca^\varepsilon(\mathbf{v}, \mathbf{v}).$$

The conclusion follows.

Lemma *The estimate*

$$|\int_\Omega F_3 v_3 d\mathbf{y}| \leq ca^\varepsilon(\mathbf{v}, \mathbf{v})^{1/2}$$

holds true for a certain $c > 0$ independent of ε and $\mathbf{v} \in \mathbf{V}$.

Now, taking $\mathbf{v} = \mathbf{u}^\varepsilon$ we get the energy estimate:

Lemma *Let $\mathbf{u}^\varepsilon$ be the solution of Π_ε. The estimates*

$$\|\gamma^\varepsilon_{\alpha\beta}(u^\varepsilon)\| \leq C \qquad \alpha, \beta = 1, 2 \qquad \|\partial_1 u_1^\varepsilon\|^2_{L^2(\Omega)} \leq C$$

$$\|\eta^{-1}\frac{1}{2}(\partial_2 u_1^\varepsilon + \partial_1 u_2^\varepsilon)\|^2_{L^2(\Omega)} \leq C \qquad \|\eta^{-2}(\partial_2 u_2^\varepsilon + u_3^\varepsilon)\|^2_{L^2(\Omega)} \leq C$$

$$\|\partial_2^2 u_3^\varepsilon\|^2_{L^2(\Omega)} \le C \qquad \|\eta\partial_1\partial_2 u_3^\varepsilon\|^2_{L^2(\Omega)} \le C \qquad \|\eta^2\partial_1^2 u_3^\varepsilon\|^2_{L^2(\Omega)} \le C$$

hold true for a certain $C > 0$ independent of ε.

We shall need an estimate on u_2^ε itself. We shall obtain it by differentiating with respect to y_2 and integrating in y_1.

Lemma *Let $\mathbf{u}^\varepsilon$ be the solution of Π_ε. The estimates*

$$\|u_1^\varepsilon\|_{H^1((0,l_1);L^2(0,l_2))} \le C \qquad \|u_2^\varepsilon\|_{\widetilde{H}_0^1((0,l_1);H^{-1}(0,l_2))} \le C \qquad \|u_3\|^2_{L^2((0,l_1);H^2(0,l_2))} \le C,$$

holds true for a certain $C > 0$ independent of ε, where

$$\widetilde{H}_0^1((0,l_1);H^{-1}(0,l_2)) = \{w \in H^1((0,l_1);H^{-1}(0,l_2)) \text{ such that } w(0,\cdot) = 0\}.$$

A first result of convergence is

Lemma *Let $\mathbf{u}^\varepsilon$ be the solution of Π_ε. The following convergences (as $\varepsilon \to 0$) hold true (in the sense of subsequences, the limits being not necessarily unique):*

$$u_1^\varepsilon \to u_1^* \quad \text{weakly in } \widetilde{H}_0^1((0,l_1);L^2(0,l_2)) \qquad u_2^\varepsilon \to u_2^* \quad \text{weakly in } \widetilde{H}_0^1((0,l_1);H^{-1}(0,l_2))$$

$$u_3^\varepsilon \to u_3^* \quad \text{weakly in } L^2((0,l_1);H^2(0,l_2))$$

where $\mathbf{u}^* = (u_1^*, u_2^*, u_3^*)$ are distributions on Ω, belonging to the spaces specified

$$\partial_2 u_1^* + \partial_1 u_2^* = 0$$

$$\partial_2 u_2^* + u_3^* = 0.$$

Finally,

$$\gamma^{\varepsilon}_{\alpha\beta}(\mathbf{u}^{\varepsilon}) \to \gamma^{*}_{\alpha\beta} \qquad \textit{weakly in } L^2(\Omega), \quad \alpha,\beta = 1,2,$$

for some $\gamma^{*}_{\alpha\beta} \in L^2(\Omega)$.

4. Limit problem and convergence in the basic problem.

Let us define the space $\mathbf{G}$ for the definition of the limit problem:

$$\mathbf{G} = \{\mathbf{v} = (v_1, v_2, v_3) \in \widetilde{H}^1_0((0,l_1); L^2(0,l_2)) \times \widetilde{H}^1_0((0,l_1); H^{-1}(0,l_2)) \times L^2((0,l_1); H^2(0,l_2)),$$

$$\partial_2 v_1 + \partial_1 v_2 = 0, \quad \partial_2 v_2 + b v_3 = 0\},$$

where we observe that v_1 defines completely v_2 and then v_3.

Clearly, $\mathbf{G}$ is a Hilbert space with the norm

$$\begin{cases} \|\mathbf{v}\|^2_{\mathbf{G}} = \|v_1\|^2_{\widetilde{H}^1_0((0,l_1);L^2(0,l_2))} + \|\partial^2_2 v_3\|^2_{L^2(\Omega)} \\ \simeq \|\partial_1 v_1\|^2_{L^2(\Omega)} + \|\partial^3_2 v_2\|^2_{L^2(\Omega)} \end{cases}$$

Remark *A straightforward comparison with the space* $\mathbf{V}$ *shows that the space* $\mathbf{G}$ *for the limit problem incorporates the two constraints corresponding to the "penalty terms" in* Π_ε *whereas the boundary conditions for* u_3*, which are concerned with the "singular perturbation terms" in* Π_ε *are lost.*

It is worthwhile to state an equivalent definition of the space $\mathbf{G}$ where the functions are defined in terms of a scalar "potential ψ":

Lemma *The space* $\mathbf{G}$ *may equivalently be defined as the space of the triplets* $\mathbf{v} = (v_1, v_2, v_3)$ *such that:*

$$v_1 = \partial_1 \psi, \qquad v_2 = -\partial_2 \psi, \qquad v_3 = -\partial_2^2 \psi.$$

where ψ *is an element of*

$$\widetilde{G} = \tilde{H}_0^2((0, \mathrm{l}_1); L^2(0, \mathrm{l}_2)) \cap L^2((0, \mathrm{l}_1); H^4(0, \mathrm{l}_2))$$

where

$$\tilde{H}_0^2((0, \mathrm{l}_1); L^2(0, \mathrm{l}_2)) = \{\psi \in H^2((0, \mathrm{l}_1); L^2(0, \mathrm{l}_2)); \psi(0, y_2) = \partial_1 \psi(0, y_2) = 0\}.$$

Remark The introduction of the scalar potential φ seems to be new in the shell literature.

D. Caillerie, A. Raoult and E. Sanchez Palencia, On internal and boundary layers with unbounded energy in thin shell theory. Parabolic characteristic and non-characteristic cases, *Asymptotic Analysis* **46** (2006), 221-249.

Some closed, but different, ideas can be associated with the *stress function* introduced by G.B. Airy (1801-1892)

It should prove useful to prove a lemma on density in $\mathbf{G}$.

Lemma *The subspace of* $\mathbf{G}$ *formed by the elements* $\mathbf{v} = (v_1, v_2, v_3)$ *which are smooth, vanish in a neighborhood of* $\{0\} \times [0, \mathrm{l}_2]$ *and derive from a "potential"* ψ *is dense in* $\mathbf{G}$.

We are now defining the limit problem. It involves the numerical coefficient $1/C_{1111}$, and B^{2222} where $C_{\alpha\beta\lambda\mu}$ is the matrix inverse of $A^{\alpha\beta\lambda\mu}$, i. e. the matrix of membrane compliances, and $\mathbf{B}$ is the matrix of flection rigidities. They are both strictly positive.

$$\tilde{\gamma}_{\lambda\mu}(\tilde{\mathbf{u}}) = C_{\lambda\mu\alpha\beta} \tilde{T}^{\beta\alpha}(\tilde{\mathbf{u}})$$

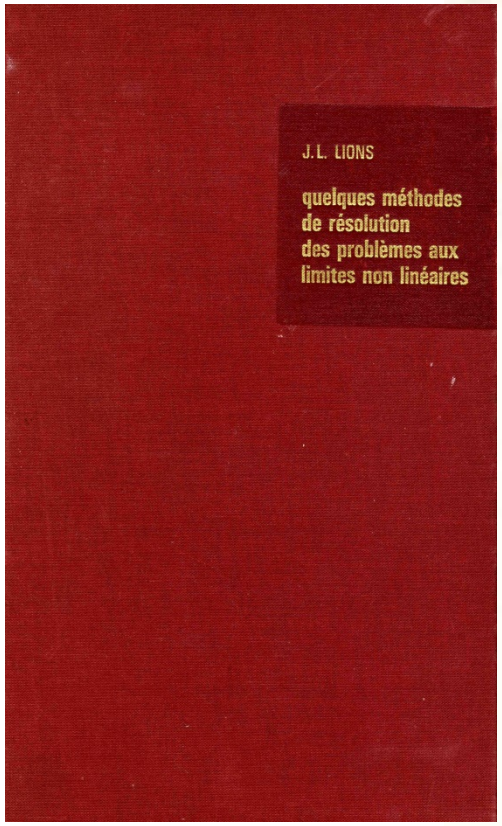

L'idée générale de la régularisation elliptique est la suivante : soit à résoudre la classique équation de la chaleur :

$$\frac{\partial u}{\partial t} - \Delta u = f \text{ dans } Q, \tag{1.1}$$

avec $u(x, 0) = 0$, $u = 0$ sur Σ.

On « *approche* » l'équation (1.1) par l'équation *elliptique*

$$-\varepsilon \frac{\partial^2 u_\varepsilon}{\partial t^2} + \frac{\partial u_\varepsilon}{\partial t} - \Delta u_\varepsilon = f \text{ dans } Q, \varepsilon > 0, \tag{1.2}$$

les conditions aux limites existantes étant maintenues et en *ajoutant* une condition aux limites pour $t = T$.

On résout (1.2) (par des « méthodes elliptiques ») puis l'on passe à la limite ($\varepsilon \to 0$).

J.-L. Lions (CIME 1963),.., O. A. Oleinik (1966), C. Bardos- H. Brezis (1968),…

Problem Π_0. *Find* $\mathbf{u} \in \mathbf{G}$ *such that*

$$\int_\Omega \frac{1}{C_{1111}} \partial_1 u_1 \partial_1 v_1 d\mathbf{y} + \int_\Omega B^{2222} \partial_2^2 u_3 \partial_2^2 v_3 d\mathbf{y} = \int_\Omega F_3 v_3 d\mathbf{y}.$$

$\forall \mathbf{v} \in \mathbf{G}$, *or equivalently, in terms of the potential, find* $\varphi \in \widetilde{G}$ *such that*

$$\int_\Omega \frac{1}{C_{1111}} \partial_1^2 \varphi \partial_1^2 \psi d\mathbf{y} + \int_\Omega B^{2222} \partial_2^4 \varphi \partial_2^4 \psi d\mathbf{y} = -\int_\Omega F_3 \partial_2^2 \psi d\mathbf{y},$$

$\forall \psi \in \widetilde{G}$.

Obviously, this problem is in the Lax - Milgram framework, as the right hand side is a continuous functional on $\mathbf{G}$. We then have

Theorem *Under the assumption* $F_3 \in L^2(\Omega)$, *Problem* Π_0 *has a unique solution.*

Our main convergence result is:

Theorem *Let* $\mathbf{u}_\varepsilon$ *and* $\mathbf{u}$ *be the solutions of* Π_η *and* Π_0 *respectively. Then, for* $\varepsilon \downarrow 0$, *we have:*

$$\mathbf{u}^\varepsilon \to \mathbf{u}$$

In other words, the limit $\mathbf{u}^*$ *is the solution of the limit problem*

The corresponding higher order partial differential equation for φ is obviously

$$(\frac{1}{C_{1111}}\partial_1^4 + B^{2222}\partial_2^8)\varphi = -\partial_2^2 F_3.$$

parabolic according the theory of linear partial differential equations

Remark *if we define the bilinear form*

$$a^0(\mathbf{u},\mathbf{v}) \stackrel{def}{=} \int_\Omega \frac{1}{C_{1111}}\partial_1 u_1 \partial_1 v_1 d\mathbf{y} + \int_\Omega B^{2222}\partial_2^2 u_3 \partial_2^2 v_3 d\mathbf{y},$$

then the symmetry of $a^0(\mathbf{u},\mathbf{v})$ *shows that the (unique) solution* $\mathbf{u}$ *of problem* Π_0 *can be characterized as the unique element of* $\mathbf{G}$ *solving the minimization problem*

$$Min_{\mathbf{G}} J_0(\mathbf{v})$$

where

$$J_0(\mathbf{v}) = \frac{1}{2}a^0(\mathbf{v},\mathbf{v}) - \int_\Omega F_3 v_3 d\mathbf{y}.$$

We can formulate, equivalently, this property in terms of the potential φ
So, the (unique) solution $\varphi \in \widetilde{G}$ *of problem* Π_0 *can be characterized as the unique element of* $\widetilde{G}$ *solving the minimization problem*

$$Min_{\widetilde{G}} \widetilde{J}_0(\psi)$$

$$\widetilde{J}_0(\psi) = \frac{1}{2C_{1111}}\int_\Omega \left|\partial_1^2\psi\right|^2 d\mathbf{y} + \frac{B^{2222}}{2}\int_\Omega \left|\partial_2^4\psi\right|^2 d\mathbf{y} + \int_\Omega F_3\partial_2^2\psi d\mathbf{y}$$

3.1.5. The shell has an edge with slight folding …

In this section we consider a case slightly more complicated than the basic problem, when the section by $y_1 = const.$ is as sketched in Fig 2.

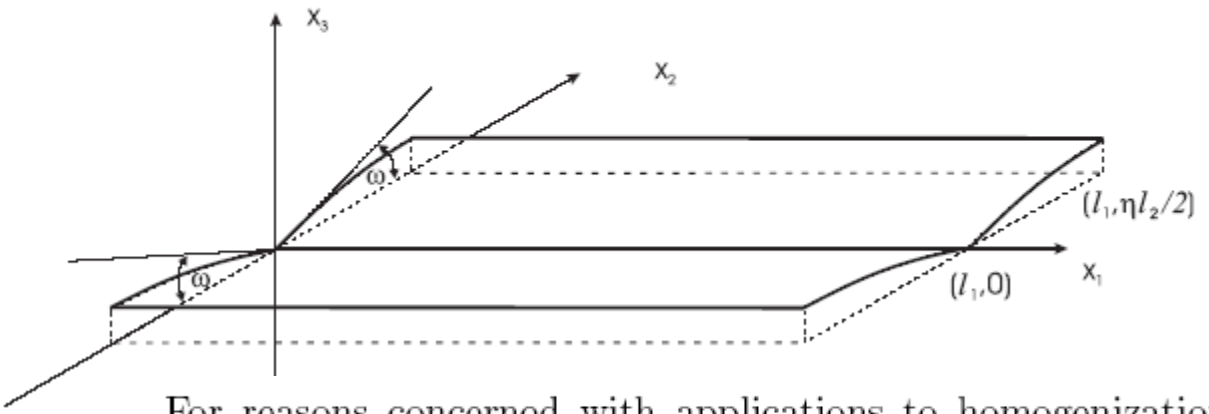

For reasons concerned with applications to homogenization problems tangent plane on $y_2 = -l_2/2$ and $y_2 = l_2/2$ is horizontal. This amounts to saying that the angle of the folding is 2ω, with $\omega = b\eta l_2/2$ (see Fig 2) where b always denote the (constant) curvature. Denoting by $\tilde{u}_i^-$ and $\tilde{u}_i^+$ the traces on $x_2 = 0$, the continuity of the displacement $\bar{\mathbf{u}}$ at the folding gives in the projections along x_1, its normal in the "base plane" and the axis Z (see Fig. 2) respectively:

In order to avoid irrelevant and cumbersome expressions, as ω is small, we shall take $cos\omega = 1$, $sin\omega = \omega$. Moreover, we shall see in the sequel that the components u_3 are asymptotically larger than u_2, and we shall neglect $\omega^2 u_2$ with respect to u_3. Then we shall consider

$$\begin{cases} \tilde{u}_1^+ = \tilde{u}_1^- \\ -\omega\tilde{u}_3^+ + \tilde{u}_2^+ = \omega\tilde{u}_3^- + \tilde{u}_2^- \\ \tilde{u}_3^+ = \tilde{u}_3^- \end{cases}$$

We consider now the case in which the shell is $2\eta l_2-$periodic with respect the section by $x_1 = const.$projected on the band $(0, l_1) \times (-\infty, +\infty)$ and having a slight folding at any section of the form $(0, l_1) \times \{k\eta l_2\}$ with $k \in \mathbb{Z}$, as sketched in Fig 3.

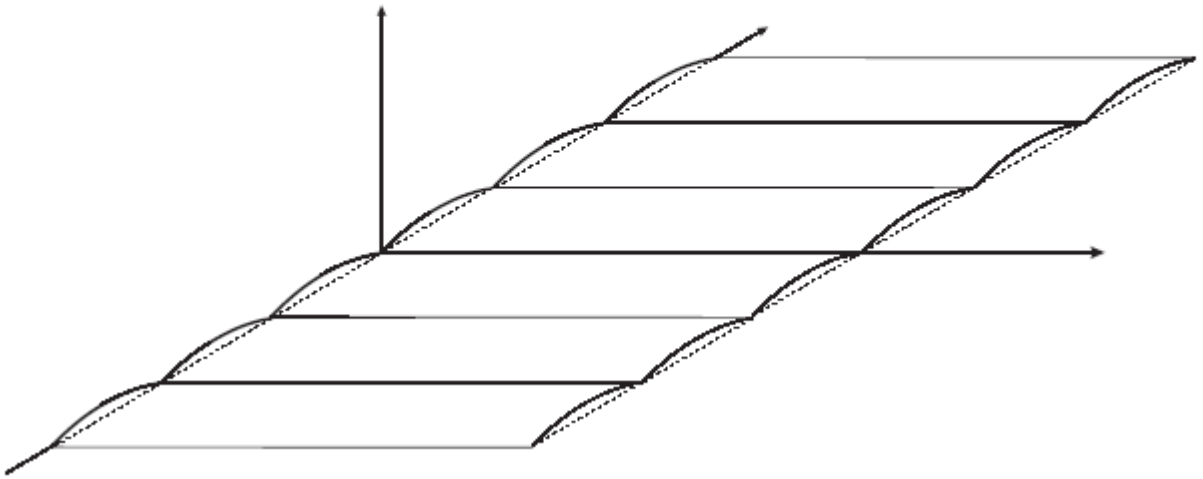

We can consider as "unit shell" the shell defied trough the rectangle $(0, l_1) \times (-\eta l_2, +\eta l_2)$, clamped along the "small sides" at $\{0\} \times [-\eta l_2, \eta l_2]$, which implies again kinematic boundary conditions similar to those indicated

We then consider periodic loadings and search for periodic solutions.

The convergence arguments follows as in previous Subsections with easy modifications.

Remark. Many other results (global properties, the obstacle problem, ...), work in progress (homogeneization, hyperbolic surfaces, ...). Many open problems.

Plan de la Subsección 3.2. Estructuras de tensegridad

3.2.2. Esculturas de Calder como punto de partida

3.2.3. Evolución por medio de otros artistas y arquitectos

3.2.4. El tema llega a las matemáticas

3.2.5. Incursión en la biología

3.2.6. Para saber más sobre tensegridades

1. Introducción.

Si esta conferencia tratase sobre Ciencia en el Arte,… recursos casi infinitos

¡¡ Sería otra conferencia distinta a esta !!

Mensaje (atípico) de esta conferencia:

Un cierto arte como origen de ciencia y tecnología

Dos mundos: **¿ dos culturas ?**

Charles Percy **Snow** (1905 –1980)

The Two Cultures and A second Look, Cambridge University Press. 1962,

(*Las dos culturas y un segundo enfoque*, Alianza, Madrid, 1977).

2. Esculturas de Calder como punto de partida

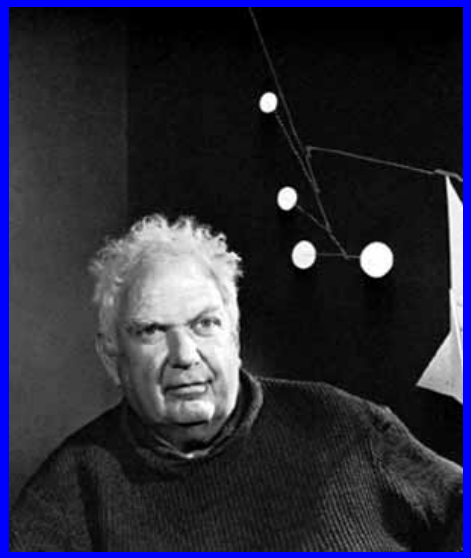

Alexander Calder

(1898 –1976)

http://calder.org

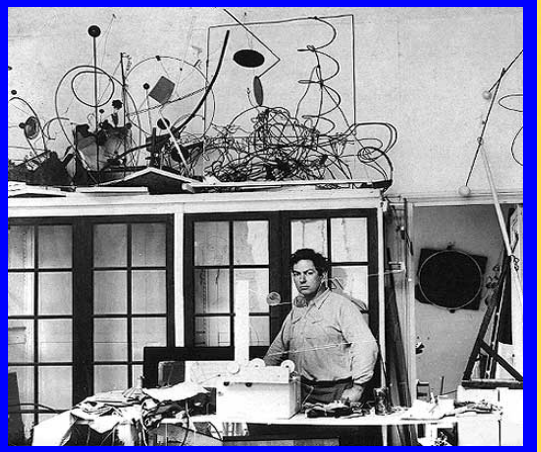

Wire sculpture, 1928.

Ligereza

Inestabilidad

Movimiento (Arte cinético)

Gravedad y viento ("formas que gravitan")

Varillas y cuerpos sólidos

Influencia de Miró, lenguaje abstracto,…

3. Evolución de una nueva concepción por otros artistas y arquitectos

Kenneth Snelson (1927-),

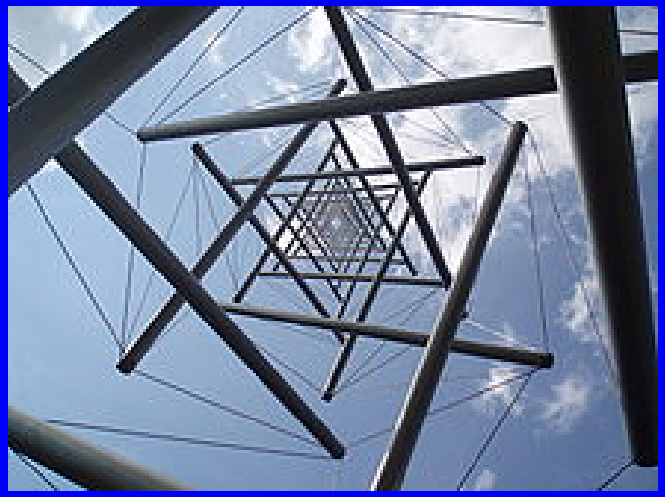

Primeras “esculturas” en 1949

(1999) Lifetime Achievement in Contemporary Sculpture Award, International Sculpture Center.

http://en.wikipedia.org/wiki/Kenneth_Snelson

Ligereza

Varillas y cuerpos sólidos ***Armazones de cables y barras***

Estabilidad: rígidez

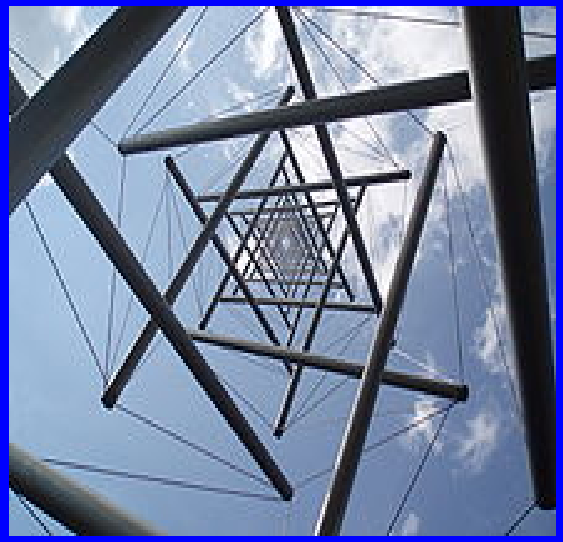

Lenguaje nuevo, muy estricto, creado por el propio artista: aparentemente inexistente en la naturaleza,…

Los únicos elementos son cables y barras flotantes, **no conectadas entre sí,**

en compresión,
frente a unos ***cables tensados*** que sólo entran en contacto con los extremos de las barras en puntos diferentes.

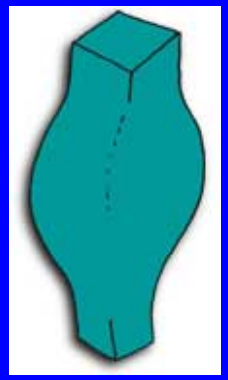

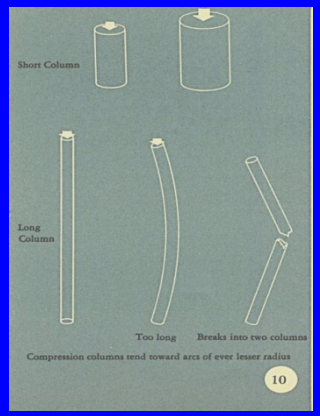

Compresión: fuerza contra una parte de una estructura.

Sección limitada con respecto a la longitud (L. Euler 1744)

Tensión: “tirar de los extremos” de una parte de una estructura.

Sección ilimitadamente pequeña con respecto a la longitud

Easy Landing (K. Snelson, 1977), Baltimore (Maryland, USA)

Todo comenzó en un curso de verano:

http://www.bmcproject.org/Biographies/SNELSON

1948 Summer Session in the Arts (University of Oregon, Campus de Eugene)

Aquel Summer Course de 1948 fue un punto de encuentro de gran trascendencia

Two weeks into the session “this strange man Buckminster Fuller arrived.”

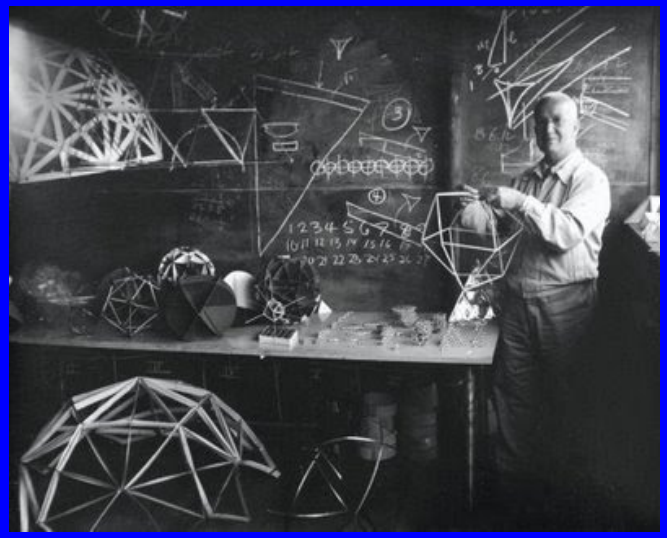

Richard Buckminster Fuller

"*Bucky*" (1895-1983)

Recuerdense las fechas:
Calder (1898 –1976)

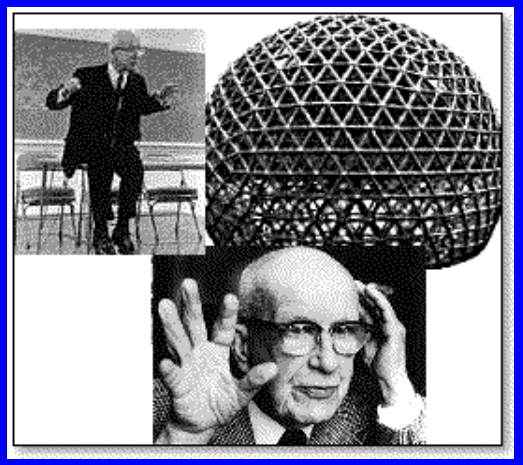

Ingeniero polifacético (arquitecto, ecologista, inventor-constructor, matemático, …)

Excéntrico, mesiánico, provocador,…

Objeto de numerosos libros, artículos, exposiciones, distinciones, …

¡¡ Otra (densa) conferencia distinta a esta !!

Abundante información en

BUCKMINSTER FULLER INSTITUTE

http://www.bfi.org/

Ley de invarianza de ángulos de Fuller:

si restamos a la suma de los ángulos convergentes en torno a todos los vértices de cualquier sistema, el número de vértices multiplicado por 360 grados, la diferencia siempre es 720 grados

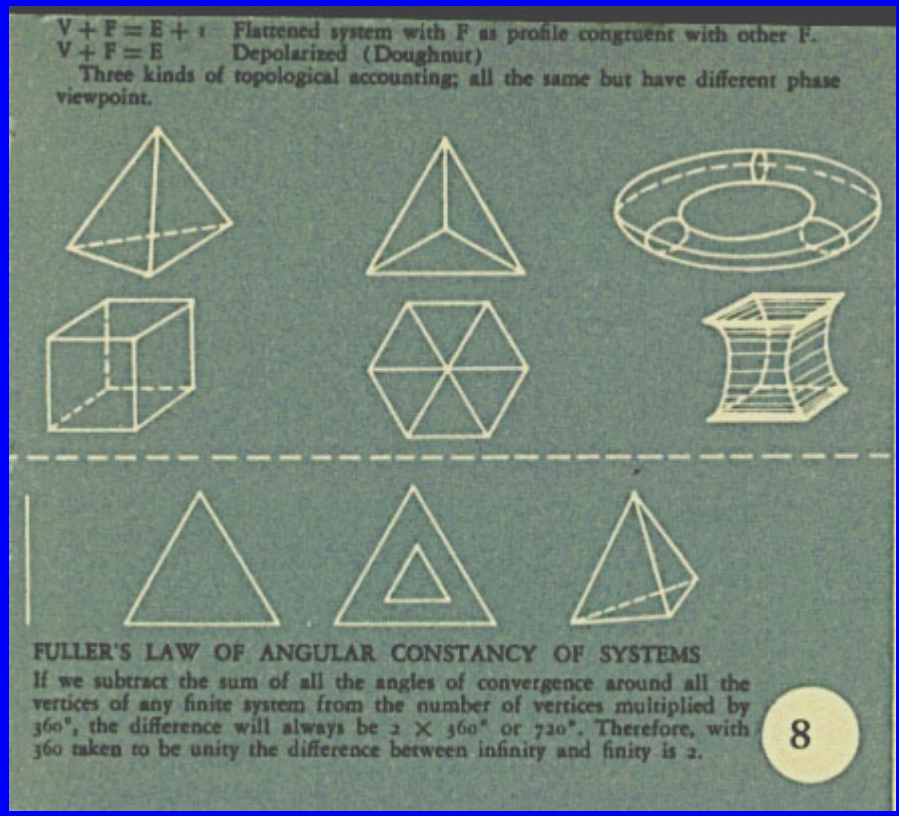

Relación con las esculturas de varillas y cables de K. Snelson

Bucky's Big Ideas

Buckminster Fuller spent his life working across multiple fields, such as architecture, design, geometry, engineering, science, cartography and education, in his pursuit to make the world work for 100% of humanity. Fuller insisted on resisting monikers of specialization to describe his work, preferring instead to describe his output as that of a 'comprehensive anticipatory design scientist ' - 'an emerging synthesis of artist, inventor, mechanic, objective economist and evolutionary strategist.' This approach resulted in the creation of numerous artifacts that cross boundaries and defy normal categorization. For the purposes of conveying Fuller's work to the uninitiated , we have organized an overview of the major themes and resulting project ideas that occupied Fuller's imaginative space:

Geodesic Domes

R. Buckminster Fuller spent much of the early 20th Century looking for ways to improve human shelter by applying modern technological know-how to shelter construction, making shelter more comfortable and efficient, and making shelter available to a greater number of people. Read more

Dymaxion World

At the heart of Buckminster Fuller's Dymaxion concept is the idea that rational action in a rational world demands the most efficient overall performance per unit of input. His Dymaxion structures, then are those that yield the greatest possible efficiency in terms of available technology. Read more

World Game

In the 1960's Buckminster Fuller proposed a "great logistics game" and "world peace game" (later shortened to simply, the "World Game") that was intended to be a tool that would facilitate a comprehensive, anticipatory, design science approach to the problems of the world. Read more

Synergetics

Synergetics is the system of holistic thinking which R. Buckminster Fuller introduced and began to formulate. Synergetics is multi-faceted: it involves geometric modeling, exploring inter-relationships in the facts of experience and the process of thinking. Read more

http://synergeticists.org/

Creador de nuevos términos: **sinergia** (del griego συνεργία, «cooperación»): resultado de la acción conjunta de dos o más causas.

"synergetics": sistema de pensamiento holístico que R. Buckminster Fuller presentó y comenzó a formular. Tiene múltiples facetas: se trata de modelización geométrica, exploración de las interrelaciones en los hechos de la experiencia y el proceso de pensar. Esfuerzos para identificar y comprender los métodos que la naturaleza utiliza en la coordinación de Universo (tanto física como metafísica). Proporciona un método y una filosofía para la solución de problemas y el diseño, por lo que tiene aplicaciones en todas las áreas del quehacer humano.

Synergetics. Exhibition Catalog, Cooper Hewitt Museum of Design. 1976.

Tensegrity = *Tension* + *Integrity* (Portfolio and Art News Annual, No.4, 1961).

tensión de los cables + integridad de la estructura (o armazón resultante, en equilibrio estable).

Tensegridad: estructura que obedece al "lenguaje de Snelson".

El término ha alcanzado ya un cierto renombre (especialmente a la sombra de Buckminster Fuller) pero, a mi juicio, es muy restrictivo: ***Esculturas (o armazones) de cables y barras***

La definición (rigurosa) es muy restrictiva.

Esta escultura de Fuller NO es una tensegridad.

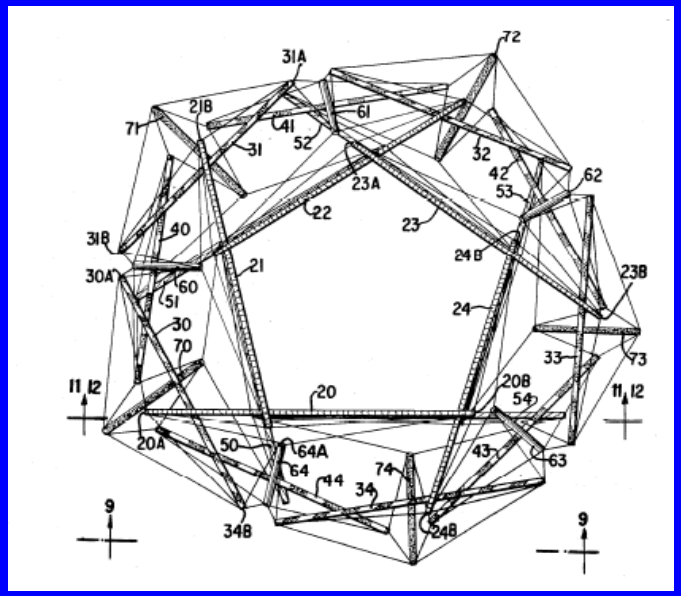

X-piece, 1948-49.

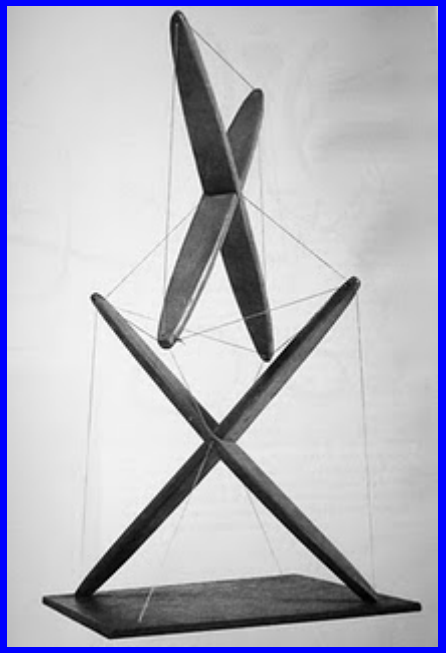

Esta escultura de Snelson NO es una tensegridad.

Patente de Fuller en EE.UU. 1973; *Non-symmetrical tension-integrity structure Patent.*

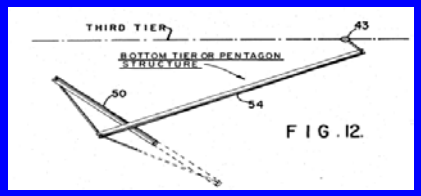

Varillas aisladas

Compresión discontinua, tensión-continua (*islas de compresión en lagos de tensión:* K. Snelson).

Controversia con K. Snelson

¿Influencia de Calder?

Mástil de la 4D/ Dymaxion House Patent 1927

¿Influencia de Fuller sobre Calder?

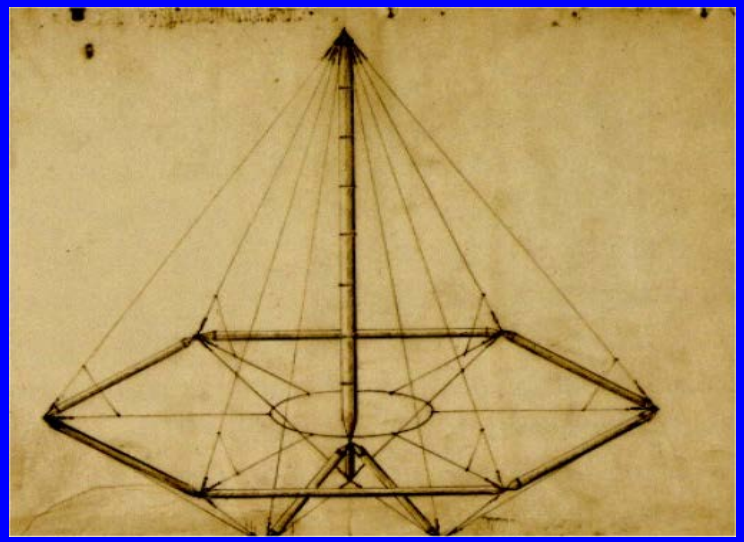

Fuller llevó sus ideas a la arquitectura originando bellas estructuras inspiradas en las tensegridades tales como, por ejemplo, su famosa *Biosphere* instalada en la Expo de Montreal de 1976.

Fuller tuvo una notable Influencia sobre Norman Foster (1935 -)

Sainsbury Centre for Visual Arts, University of East Anglia in Norwich, Norfolk, UK. 1974-1978

5.328 Toneladas

How Much Does Your Building Weigh, Mr Foster?

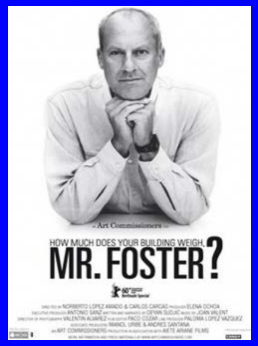

Documental, 78 minutos
Directores: Norberto López Amado y Carlos Carcas,
Estrenado el 8 de Octubre de 2010

Hacer más con menos (Fuller)

Menos es más, Ludwig Mies van der Rohe (1886–1969),

Hearst Tower, New York, 2007.

El impacto de Fuller (en particular de su **cúpula geodésica**) alcanzó incluso a un ámbito tan aparentemente lejano como el de la Química.

Año Internacional de la QUÍMICA 2011

Los **fulerenos** (fullerenes) son la tercera forma más estable del carbono, tras el diamante y el grafito.

El primer fulereno se descubrió en 1985 y se han vuelto populares entre los químicos, tanto por su belleza estructural como por su versatilidad para la síntesis de nuevos compuestos, ya que se presentan en forma de esferas, elipsoides o cilindros.

Los fulerenos esféricos reciben a menudo el nombre de *buckyesferas* y los cilíndricos el de *buckytubos*.

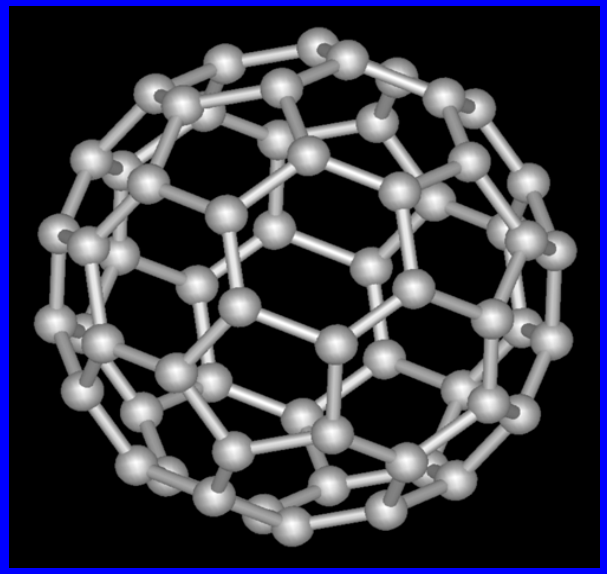

El más conocido es el **buckminsterfulereno:** formado por 60 átomos de carbono (C60), en el que ninguno de los pentágonos que lo componen comparten un borde; se asemeja a un balón de fútbol (domo geodésico), constituido por 20 hexágonos y 12 pentágonos, con un átomo de carbono en cada una de las esquinas de los hexágonos y un enlace a lo largo de cada arista.

4. El tema llega a las matemáticas

El lenguaje de lo “casi intangible”

Crab Canon on a Möbius Strip.

http://www.youtube.com/watch?v=xUHQ2ybTejU

Canon Cangrejo [*Quaerendo invenietis*], de Ofrenda Musical,

J. S. Bach (1747).

D. Hofstadter: *Gödel, Escher, Bach* (1979)

El libro de la naturaleza está escrito en lenguaje matemático

Galileo Galilei (1564-1642)


DIALOGO
DI
GALILEO GALILEI LINCEO
MATEMATICO SOPRAORDINARIO
DELLO STVDIO DI PISA.
E Filosofo, e Matematico primario del
SERENISSIMO
GR. DVCA DI TOSCANA.
Dove ne i congressi di quattro giornate si discorre sopra i due
MASSIMI SISTEMI DEL MONDO
TOLEMAICO, E COPERNICANO,
Proponendo indeterminatamente le ragioni Filosofiche, e Naturali
IN FIORENZA, Per Gio. Batista Landini M.DC.XXXII.
CON LICENZA DE' SUPERIORI.

Man Ray (1890 - 1976) (e.d. Emmanuel Rudzitsky)

Quedó impresionado por la materialización de las ecuaciones matemáticas tras una visita al *Institut Henri Poincaré* de París, en 1935.

Shakespearian Equation: objets mathématiques (1935-1948): colección de fotos y pinturas

Mathematical Object: Ruled Surface, 1936

Shakespearean Equation: Twelfth Night, 1948

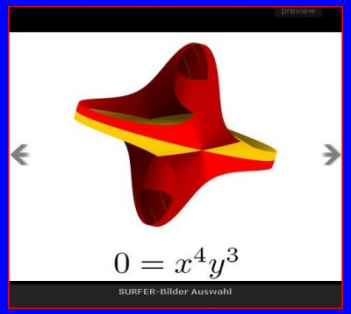

Imaginary 2011

Real Academia de Ciencias:

19 de octubre a 15 de noviembre 2011

(Centenario de la RSME)

La posibilidad de experimentar fácilmente con esas estructuras, atrajo tempranamente a numerosos matemáticos (Robert Connelly (1947-), …).

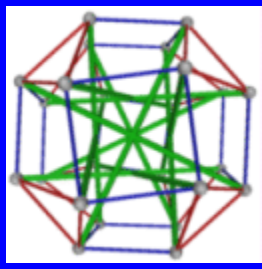

http://www.math.cornell.edu/~connelly/

El primero de los matemáticos españoles: Miguel de Guzmán Ozamiz (1936-2004),

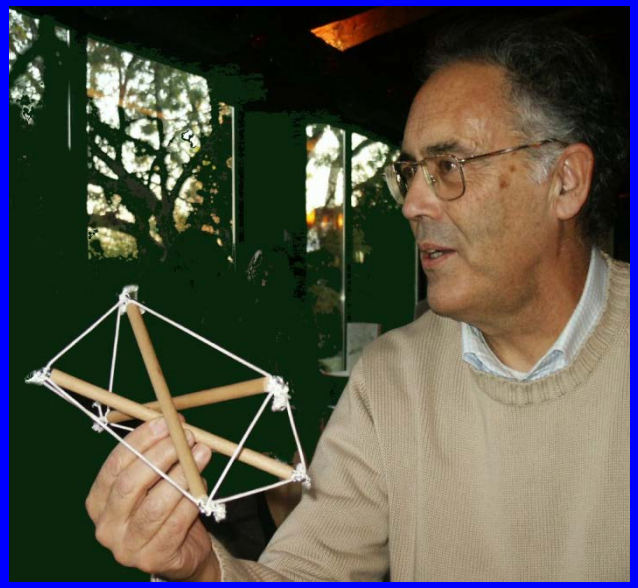

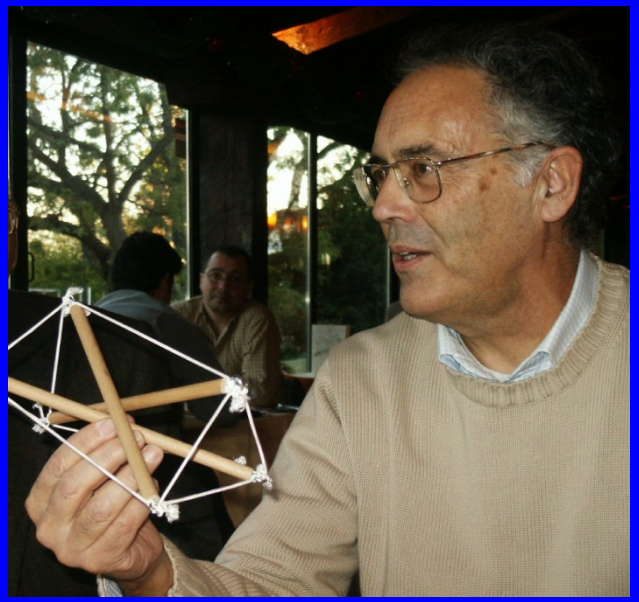

Tenía muy avanzado un proyecto de libro sobre *Tensegridades*, habiendo construido una cantidad importante de esas *estructuras* con las que experimentaba, disfrutaba y hacía disfrutar a numerosas personas.

Miguel de Guzmán introdujo su propia definición de tensegridad (un poco más general que la de Sneldon y Fuller):

"Consideremos una configuración geométrica constituida por un número finito de puntos y por unos cuantos segmentos que unen esos puntos.

Una ***estructura de tensegridad*** consiste en asignar vectores a los puntos, en las direcciones de los segmentos que concurren en ellos de forma que:

(a) la resultante en cada punto es nula,
(b) para cada segmento, la suma de los vectores asignados a sus extremos es cero"

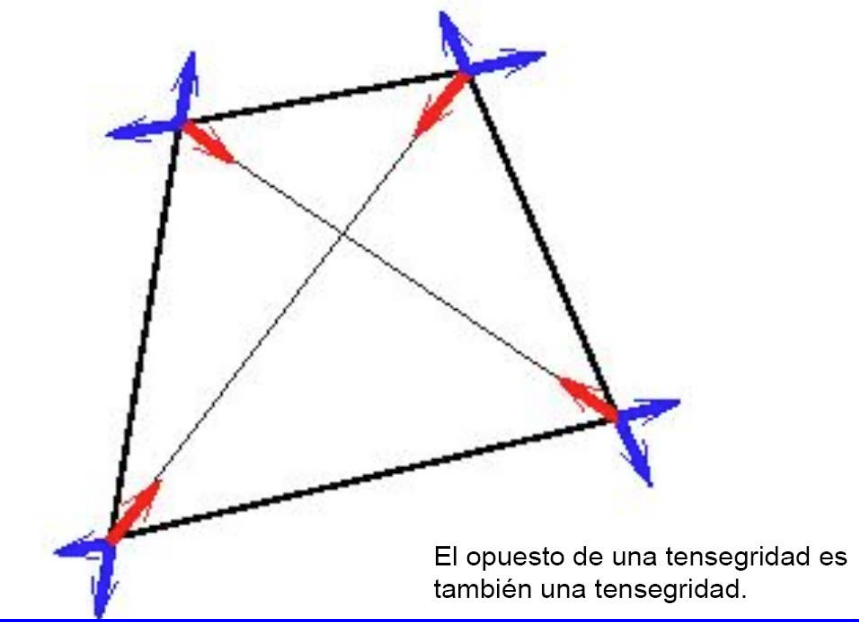

El opuesto de una tensegridad es también una tensegridad.

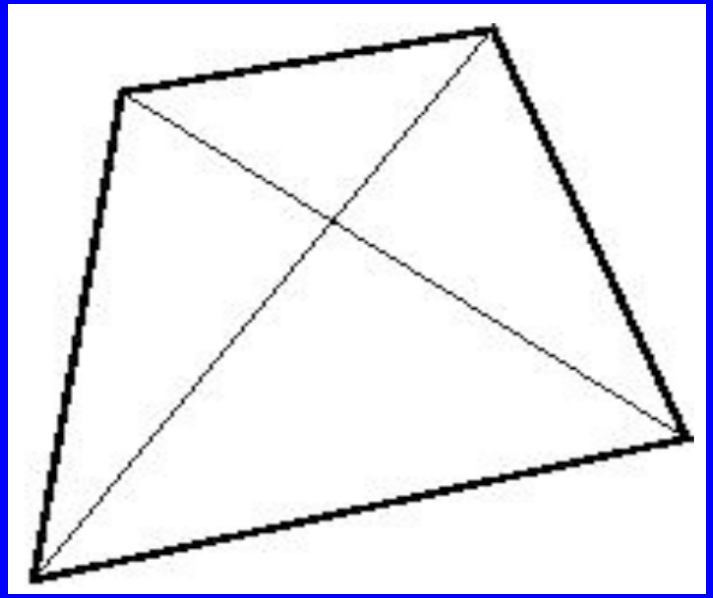

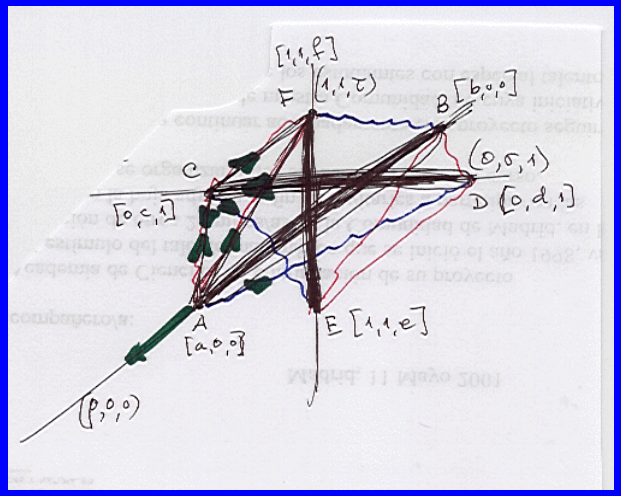

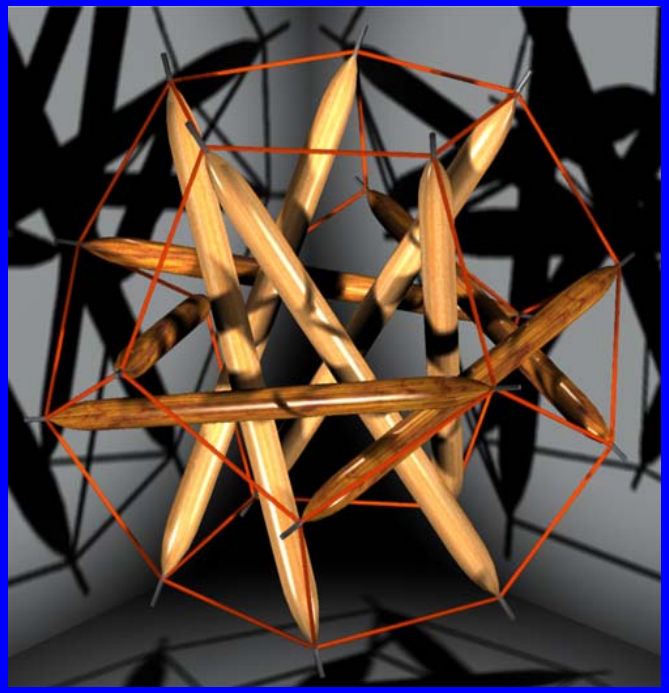

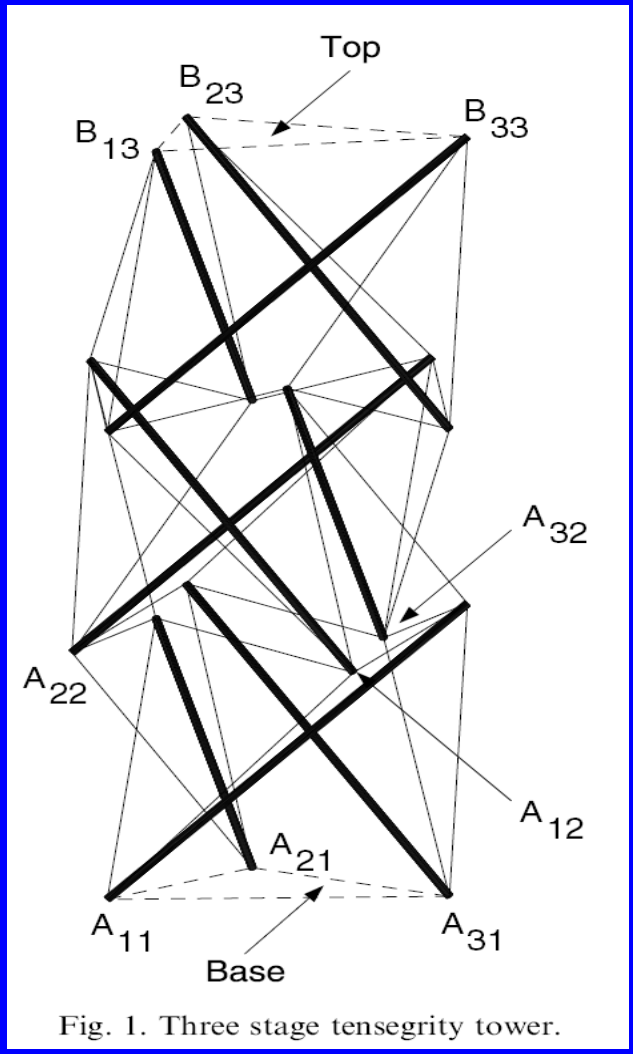

Fig. 1. Three stage tensegrity tower.

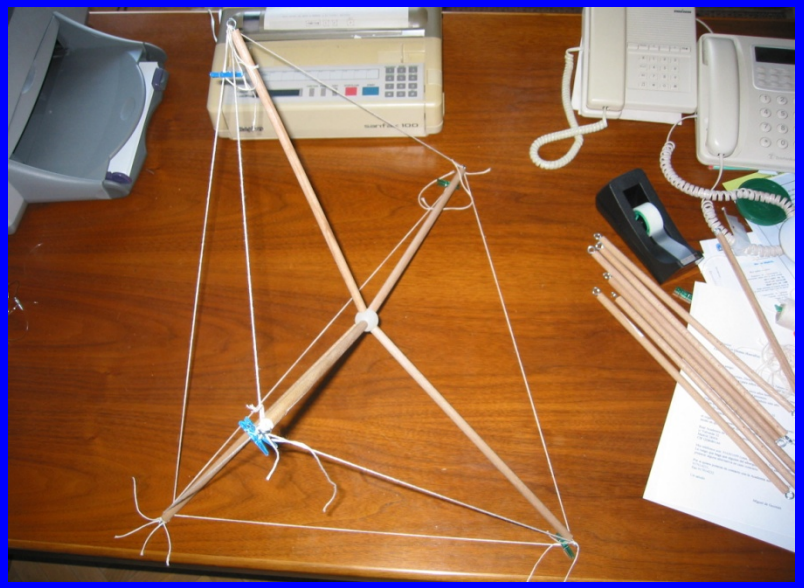

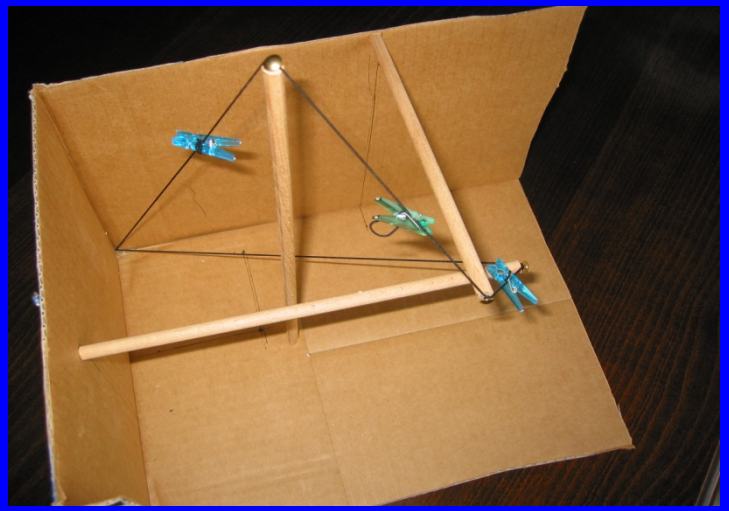

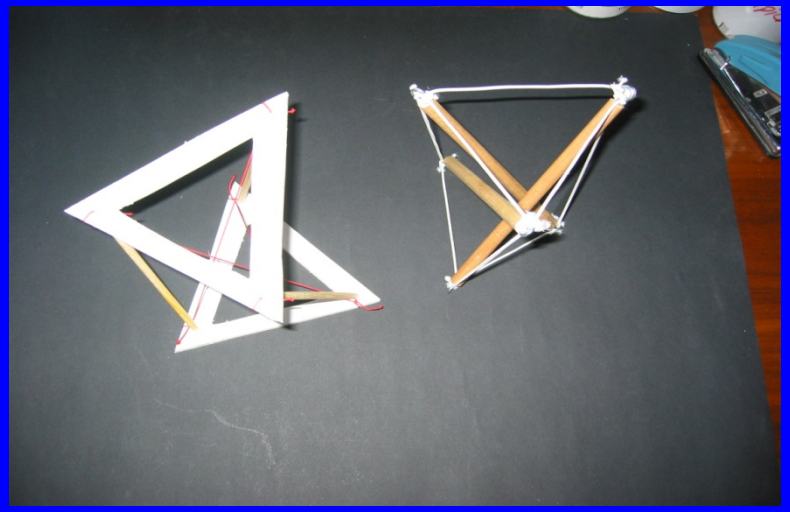

Desde el punto de vista matemático son numerosas las cuestiones relacionadas con las *tensegridades*

razones de la rigidez de esas livianas estructuras

propiedades de optimización en la conexión de sus aristas

problema inverso: dados unos puntos del plano, o del espacio, hallar las condiciones que aseguran que esos puntos puedan ser las aristas de una cierta tensegridad.

Además del propio interés geométrico, las respuestas a tales cuestiones tienen relevantes consecuencias en muchos otros dominios, entre ellos el arquitectónico.

Una de las tensegridades inicialmente consideradas por K. Snelson: **el prisma oblicuo de base triangular.**

Tres barras de igual longitud separadas en el espacio, tres cables de igual longitud por cada extremo, cada cable uniendo (y separando) en el espacio los extremos de las barras en una estructura rígida autotensionada.

Simetría rotacional alrededor de un eje.

La simetría hace muy sencilla
la determinación de fuerzas (vectores).

Configuración de seis puntos en el espacio:

- Sean los puntos 1,2, 3, 4, 5, 6.
- No hay cuatro en un mismo plano. A cada punto llegan cuatro segmentos.
- Esto implica que la única configuración posible de segmentos es: 12,13,23,45,46,56,14,15,25,26,36,34.
- Es decir dos triángulos 123, 456 (en la base y la cima) y tres cuadriláteros (laterales) 1264, 2365, 1362.

Es posible explorar la situación geométrica, p.e. con Derive, Maple,Mathematica, Matlab,…

5. Incursión en la biología

Donald Ingber
(1940-)

Un punto de vista insospechado en el estudio de estas estructuras apareció con la obra de Donald Ingber, a mediados de los años 70, al reconocer estructuras muy semejantes en el esqueleto de las células .

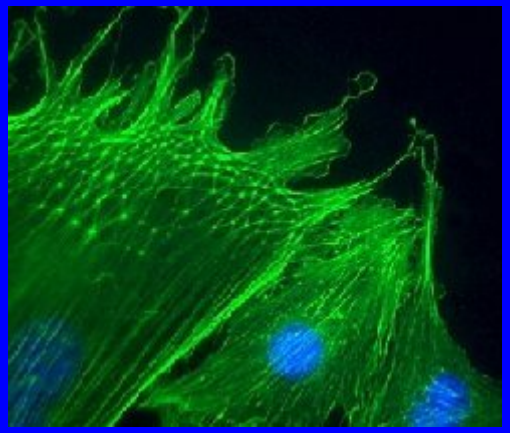

En el citoesqueleto, las cadenas de proteínas - finas, gruesas o huecas - cumplen el rol de los cables y las varillas. Todas las proteínas conectadas entre si forman una estructura estable, pero flexible.

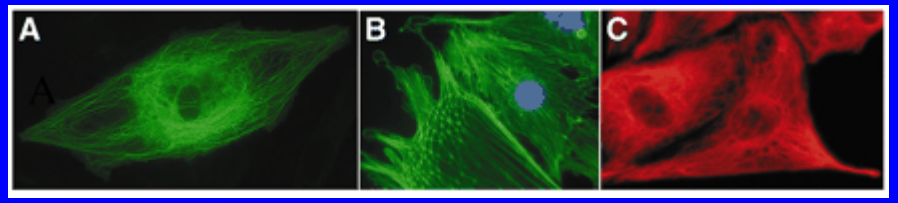

Arquitectura de la célula: microfilamentos, microtubos,..

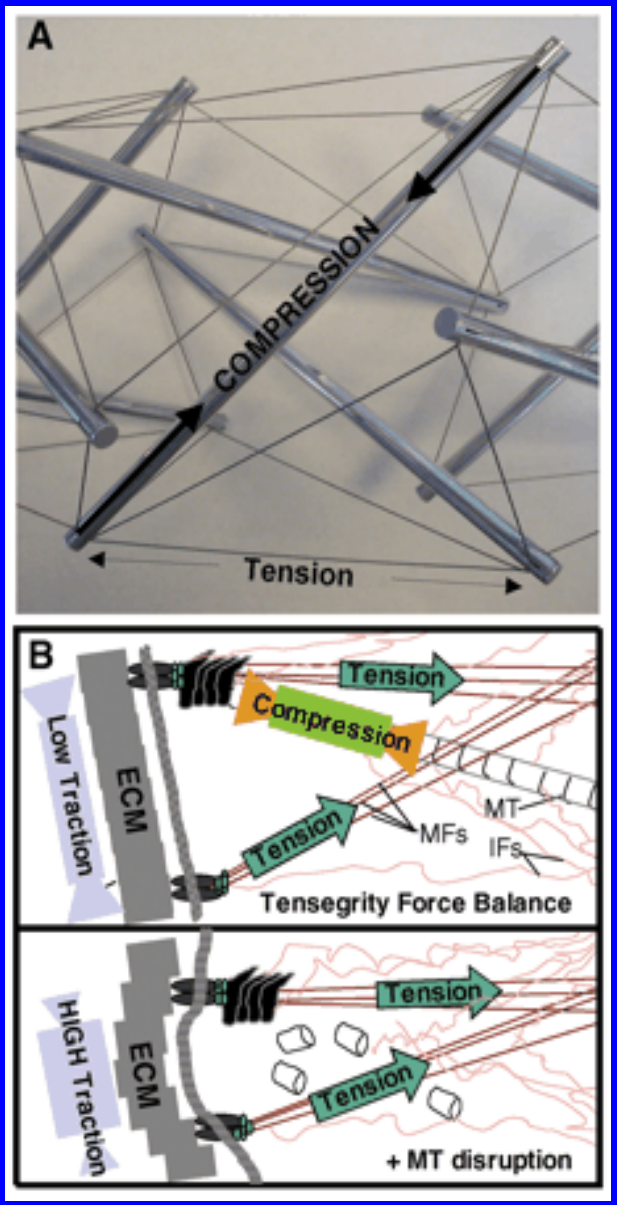

El citoesqueleto percibe la gravedad - o cualquier tipo de fuerza - a través de proteínas especiales llamadas *integrinas*, las cuales se proyectan a través de la superficie de la membrana celular“

Dentro de la célula, las integrinas están conectadas al citoesqueleto. Por fuera, están unidas a un armazón conocido como matriz ECM extracelular --una estructura fibrosa a la cual se conectan las células de nuestro cuerpo.

Diagrama esquemático del balance de fuerzas entre los microfilamentos tensionados (FMs), filamentos intermedios (FI), microtúbos comprimidos (MTs) y la ECM en una región de una matriz de tensegridad celular.

Las fuerzas de compresión soportados por microtúbulos (arriba) se transfieren a las adherencias ECM cuando se interrumpen los microtúbulos (abajo), lo que aumenta la tracción sustrato.

El esqueleto humano como tensegridad

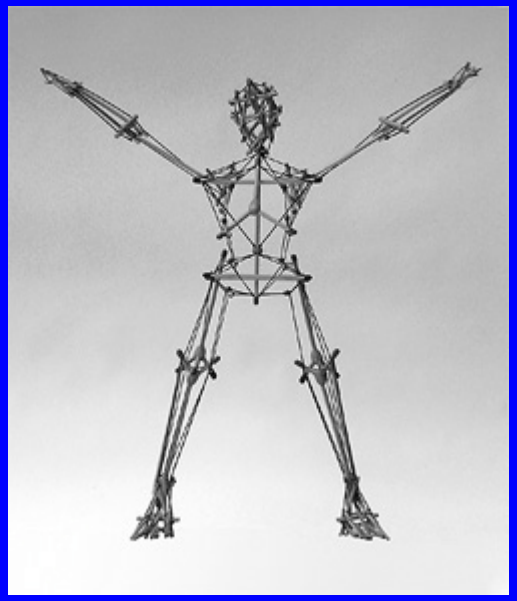

Stephen M. Levin (Oregon, USA)

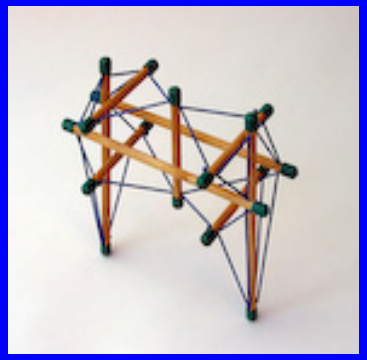

Single Tensioned Pelvis
model #05-STP-3.1

Tensegrity Spine

Regreso a la idea dinámica (cinética) de Calder

Tom Flemons (colaboró con Stephen M. Levin)

Simulaciones dinámicas del tensegridad célula

http://tensegrity.wikispaces.com/Flemons%2C+Tom

Animated Spiral Tensegrity Mast

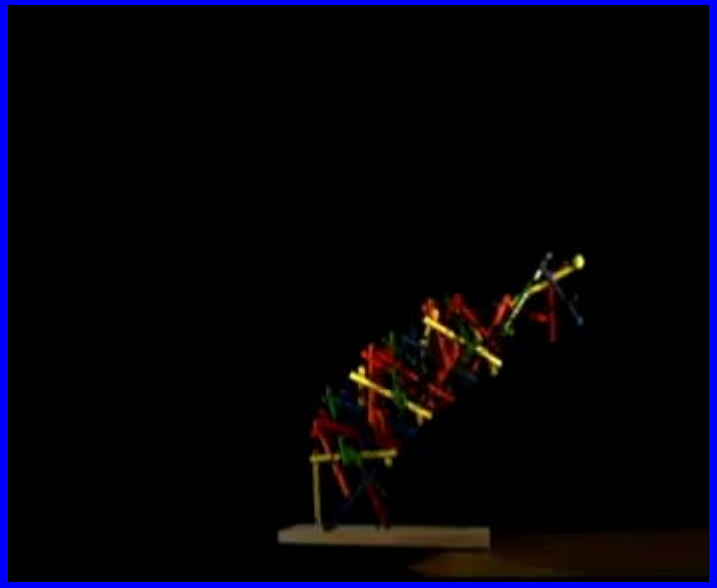

7. Para saber más

http://synergeticists.org/
http://www.tensegridad.es/

R. Motro, Tensegrity. Structural Systems for the Future, Kogan Page Science, Londres, 2003.

Valentin Gómez Jáuregui: *Tensegridad : estructuras tensegríticas en ciencia y arte*, Univ. Cantabria, 2007

José Antonio Bustelo*: Equilibrio de tensiones*, Equipo Sirus, Madrid, 2007.

M. de Guzmán y D. Orden: Finding tensegrity structures: Geometric and symbolic approaches. Proceedings of EACA-2004. pp. 167–172.

D.E. Ingber (1998) “The Architecture of Life”. *Scientific American Magazine*. Enero,1998.

D.E. Ingber(2003) “Tensegrity I. Cell structure and hierarchical systems biology”. *Journal of Cell Science*, No.116, pp.1157-1173.

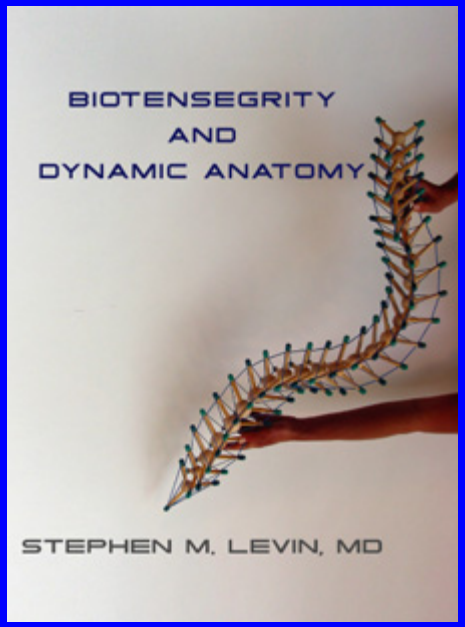

S. M. Levin, Biotensegrity and Dynamic Anatomy,

(DVD: conferencia & conversaciones con Tom Flemons)

http://www.biotensegrity.com/

4. ¿Analogías en el ámbito de la arquitectura?: Indicios ...

Ilustración de los temas de referencia:

1. Energía: climatología.

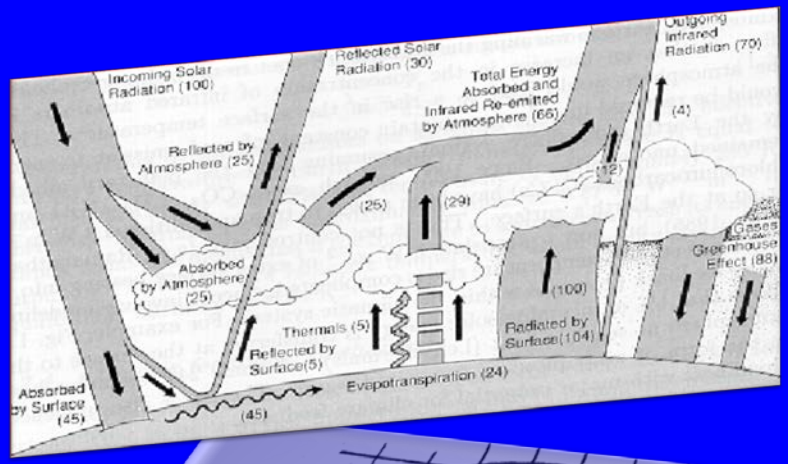

2. Materia: nuevos materiales.

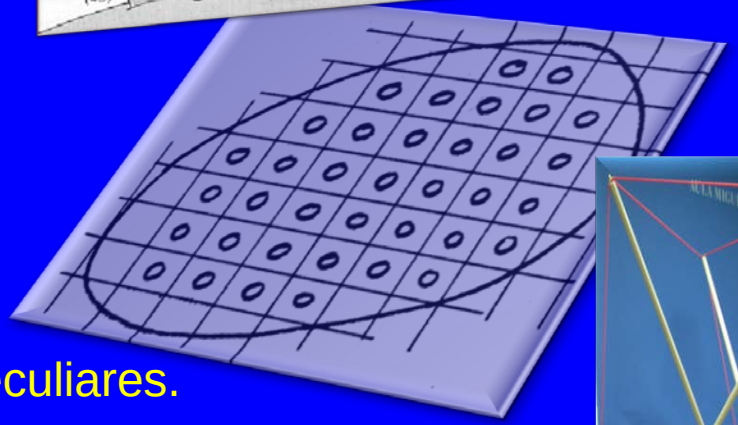

3. Geometría: estructuras elásticas peculiares.

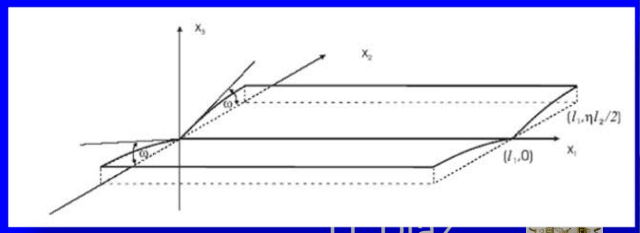

Control cimático en espacios abiertos: Expo 92

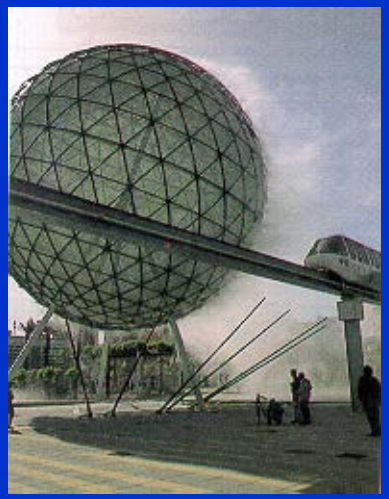

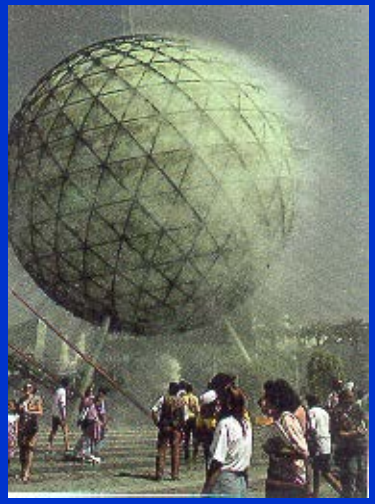

Dpto. de Ingeniería Energética y Mecánica de Fluidos,

Univ. de Sevilla

Ley de “anti-tabaco” 2008…..

Soledad Sevilla transforma el Palacio de Cristal en una bóveda celeste

La artista, pionera en el arte de la instalación, pinta el cielo en este edificio emblemático de El Retiro

ÁNGELES GARCÍA - Madrid - 10/11/2011

La instalación 'Escrito en los cuerpos celestes' de Soledad Sevilla.- MUSEO REINA SOFÍA

Pionera en el arte de la instalación, Soledad Sevilla (Valencia, 1944) ha dedicado su obra a indagar en las relaciones entre materia, luz y espacio. Interesada siempre en el mundo

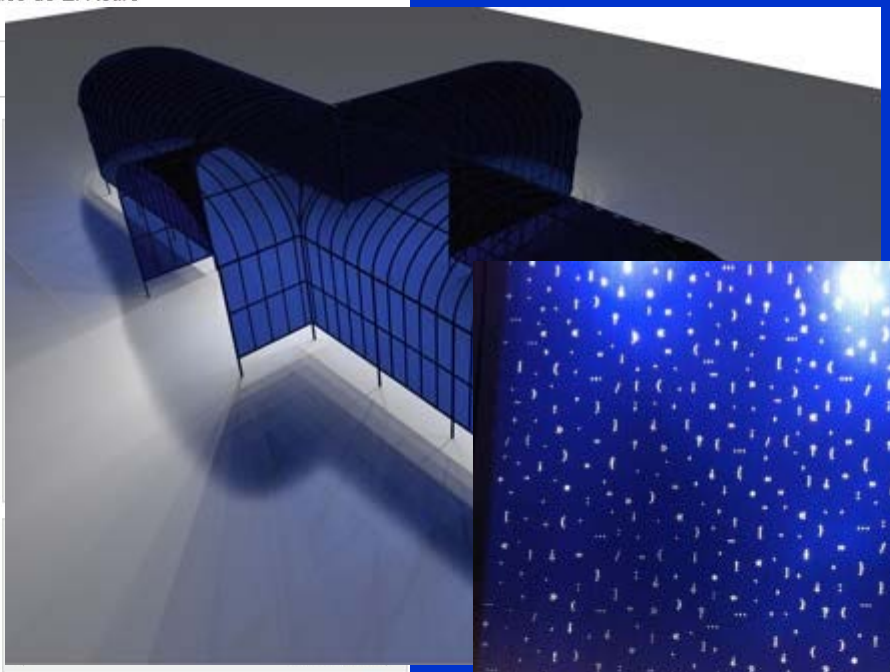

The consideration of this type of periodic structures is motivated by some of the structures designed by the outstanding engineer Eduardo Torroja (Madrid, 1899-1961).

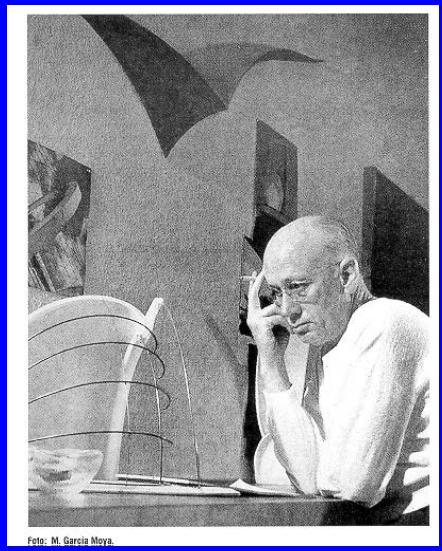

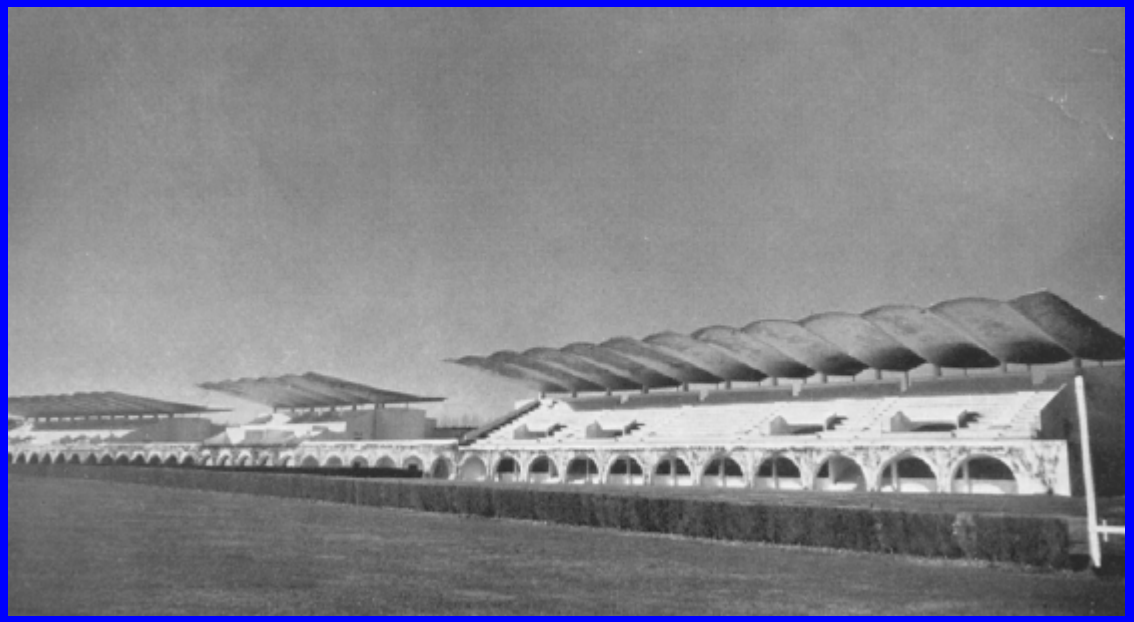

HIPÓDROMO DE LA ZARZUELA. MADRID, 1935.

C. Arniches, L. Domínguez y Eduardo Torroja. Con la empresa constructora Agroman E.C.

The shell roofs of the Madrid Racecourse (1935) are a brilliant result of the forms of the reinforced concrete consisting of a system of portal frames, spread at 5 m intervals and connected longitudinally by small reinforced concrete double curvature vaults. The cantilever roof, with a minimum thickness of 5 cm, overhangs to a distance of 12,8 m.

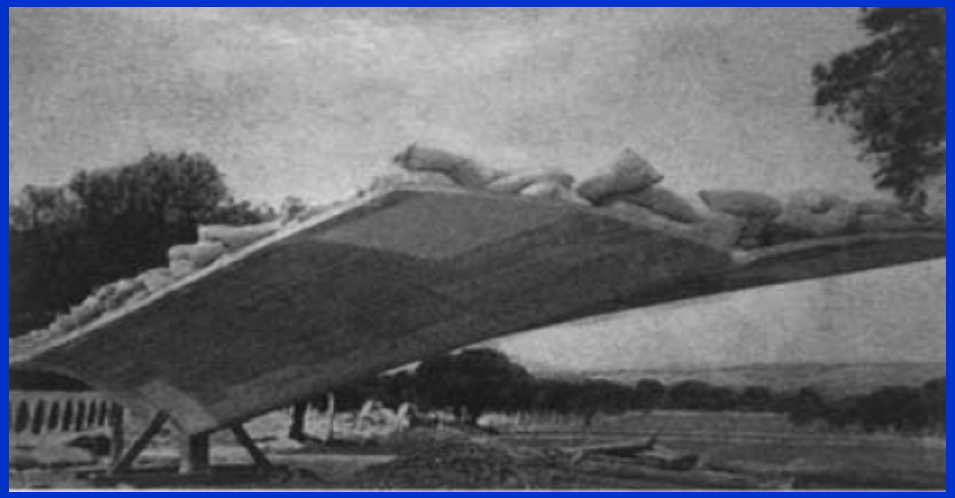

Estructuras desplegables: S. Pellegrino, Cambridge U.K.

Es lo que Chillida llamaba la “arquitectura invisible”.

Obras inspiradas en tensegridades

La nube: Neuchatel Suiza EXPO.02

Ingenieros: Passera & Pedretti

Arquitectos: Diller & Scofidio Architecture New York

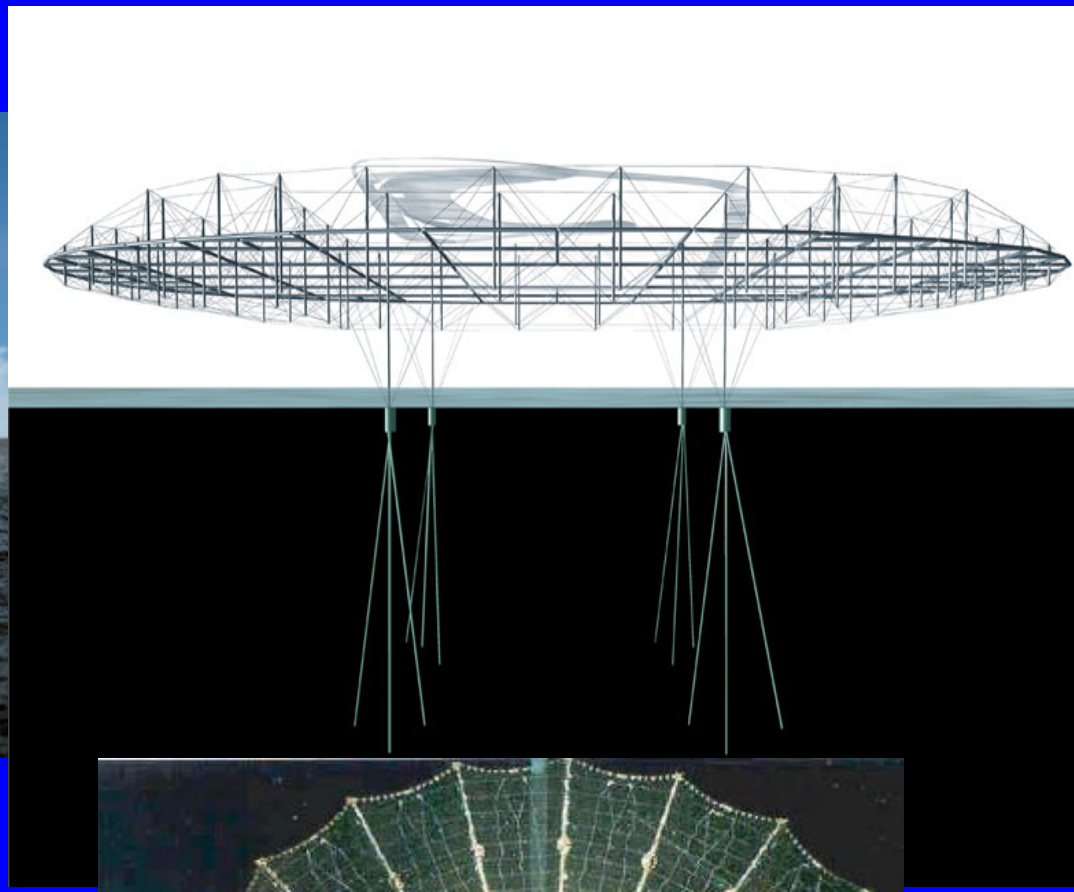

Misión Galileo (ESA) 1991

Gracias por su atención